University of Thessaly

Department of Mechanical Engineering

Failures in Marine Structures

Αστοχίες στις Θαλάσσιες Κατασκευές

Diploma Thesis

Tilemachos I. Solinis

Supervisor

Prof. G.N. Haidemenopoulos

Volos, 2023

In memory of my grandfather.

Acknowledgements

First and foremost, I would like to express my sincere gratitude to Professor Gregory Haidemenopoulos, the supervisor of my thesis, who offered me the opportunity to pursue this intriguing topic. I would also like to thank my entire family and all of my friends for their support throughout my years at the University of Thessaly.

Contents

Table of Figures

Abstract

The thesis deals with the failures in marine structures and focuses on four important failure factors that affect their operation and lifespan. Initially, a brief overview of failures is given through the listing of historical incidents, followed by a categorization of materials and a reference to failure theories that play an important role in the design of constructions and the prediction of failures. Then, marine structures are referred to, and a brief description of the process from their design to their withdrawal is presented. Subsequently, the failures that were considered as the most significant, which can affect these structures, are analyzed. Ductile and brittle fracture, corrosion, and fatigue are damage mechanisms that can cause economic, environmental, and human losses. Finally, eight case studies are studied, in which extensive reference is made to marine structures accidents, analyzing the root causes of each failure and arriving at conclusions that provide knowledge and experience that will help the evolution of the industry. The purpose of the thesis is to record, through the main types of failures, the challenges that the shipping industry has to face through their analysis.

1. Introduction

The importance of the maritime industry is highlighted by the statistics; it is responsible for the transportation of 80% of the world's trade, greatly impacting economic growth. Nearly 50,000 merchant ships are trading globally, carrying all types of cargo from various industries. Throughout recorded history, shipping has been widely utilized to connect people and transport goods from one place to another. Despite the vital role of ships, the ongoing energy demands of the world have resulted in the construction of oil platforms. These offshore structures are built to take advantage of petroleum and natural gas found in rock formations beneath the seabed. Vessels and oil rigs, among other marine structures, are operated by crews who are responsible for maintaining and operating the equipment. Moreover, these constructions must deal with harsh marine environmental conditions, especially in the open ocean.

As seen, ships and oil platforms form a complex dynamic system that is affected by various factors. In the past, the world has suffered from frightening disasters that have resulted in human loss and had a significant impact on the environment. From the RMS Titanic, which cost more than 1,500 lives, to the MV Prestige catastrophe in 2002, when an oil spill occurred off the coast of Spain - the largest environmental disaster ever in Spain and Portugal - the shipping community has been led to take action towards a safer industry.

To address the aforementioned challenges, safety measures are necessary. The maritime industry operates internationally, thus there is a need for global collaboration. In 1948, the International Maritime Organization (IMO) was established for this purpose. It is a specialized branch of the United Nations that regulates shipping, and its main goal is to develop regulations and ensure their implementation. In 1973, IMO adopted the International Convention for the Prevention of Pollution from Ships (MARPOL) with the aim of preventing and minimizing environmental pollution from ships. In 1974, IMO adopted the International Convention for the Safety of Life at Sea (SOLAS), which provides a regulatory framework for the minimum safety standards in the construction, equipment, and operation of ships. This was a result of the Titanic disaster.

It is imperative that marine structures meet a set of safety standards to prevent catastrophic accidents. These standards are related to, among other things, structural failures. During dry docking, a mandatory process for vessels every 5 years, ships and offshore platforms are taken out of the water for inspection and maintenance. The supervision of the hull's integrity covers the state of the coating, the assessment of potential structural defects, and the remaining thickness of plates. It is evident that failures play a crucial role in the structural status and should be taken into consideration, as they can lead to serious consequences.

The most frequent failures in the environment where marine structures operate are ductile fracture, including bending and buckling, brittle fracture, corrosion, and fatigue. These failures pose a challenging issue as they can lead to severe consequences, including costly repairs, loss of use, and even endangering lives. Understanding the root causes of these devastating failures and developing ways to prevent them is an essential process that ensures the safety and reliability of marine structures, which are important infrastructure of the world.

Ductile fracture is a mode of material failure that occurs when the material is subjected to high stresses above the yield stress. This means that ductile failure can result in catastrophic consequences for marine structures, as it leads to permanent deformation of the elements that undergo ductile failure, putting the structure's reliability at risk. Excessive plastic deformation can cause the rupture of critical components and, in the worst case, the total break of the ship or platform.

Brittle fracture, in contrast to ductile fracture, occurs suddenly and without prior warnings. History has shown that brittle fracture can have detrimental results, as it leads to the complete destruction of the structure and often results in human losses. This phenomenon is connected with other types of failure such as fatigue and corrosion and is exacerbated by low temperatures. The operating environment of marine structures, including saltwater and high pressure, as well as cyclic loads, puts vessels at risk and makes it a critical issue for their structure's integrity. To address this risk, it is necessary to have a thorough understanding of the mechanisms and causes of brittle fracture, as well as effective methods for estimating and mitigating its impact.

Corrosion is a natural process that occurs when a metal interacts with its environment, leading to degradation and deterioration over time. Marine structures such as ships and platforms operate in a harsh, corrosive environment, so corrosion can have a significant impact on their integrity and safety. The overall environment, including different weather conditions and exposure to saltwater, can exacerbate the phenomenon and cause detrimental effects to the structures. Corrosion occurs in various forms, each with its unique mechanism of damage that causes distinct consequences for the metal that is attacked. To prevent and mitigate the effects of corrosion, it is important to thoroughly understand the mechanisms behind it and to implement protection strategies, including regular maintenance and inspection programs.

Fatigue is another type of failure that affects the durability of the structure, leading to progressive cracking and eventual rupture. Marine structures are exposed to sources that create repeated stress cycles, such as waves, winds, and ship traffic, which are characterized as dynamic loads. These cyclic loads cause the formation and propagation of cracks, leading to fatigue damage over time. Fatigue is classified based on whether the element or structure has initial cracks or not. Understanding fatigue as a type of failure and assessing the structure's response to repeated loads is important for implementing effective design and maintenance programs to ensure the stability and safety of the structure, the environment, and the people working on them.

2. Literature Review

2.1 A briefing view of failure

The term "failure" describes the inability of a material or machine component to function safely and effectively. This means that the component or structure has become completely inoperable or is still operational but is unable to perform its intended function satisfactorily. Alternatively, it may be deemed risky to use due to its unreliability or lack of safety. Failure can be caused by changes in size, shape, or material properties, and can affect the integrity of a construction. Design flaws, manufacturing processes, and degradation mechanisms may contribute to structural failure, as well as human factors such as non-adherence to procedures, inadequate maintenance and inspection, misuse of the machine, and inadequate quality control.

Failures can have serious consequences in terms of financial losses and potential harm to people and the environment. Failures can be divided into three categories: Mechanical failures, including damage mechanisms such as excessive elastic displacement, buckling, plastic deformation, brittle fracture, and fatigue. Mechanical failures occur under a gradual increase in beam bending due to intended loading or compressive loads applied through buckling. Plasticity can cause permanent deformation and non-reversible changes in dimensions due to strong external forces that exceed the yield stress. Brittle fracture occurs suddenly and below the yield strength, while fatigue initiates and propagates cracks due to repeated cyclic loads. Mechanical failures play a crucial role in the operating life of marine structures as they impact the integrity and reliability of the structure.

The second category of failures is related to corrosion and its modes. Corrosion affects the metal surface and is a challenging mechanism as it occurs due to the interaction between the metal and its environment. Over time, corrosion can cause significant issues, so it is essential to follow a specific inspection program. The third category of failures is associated with catastrophic results when the material or structure is exposed to high temperatures. This type of failure includes phenomena such as oxidation, carburization, and sulfidation, but their effect on marine structures is not significant [1].

2.2 Historical Review

2.2.1 The Boston Molasses Disaster

In 1919, a catastrophic accident shocked Boston when a massive tank holding 2.3 million gallons of molasses burst, resulting in the death of 21 people and injuring 150 others. The tank, made of steel, was 17 meters tall and 27 meters in diameter. The explosion caused a wave of molasses to flood the streets of Boston at an estimated speed of 56 kilometers per hour. In addition to human casualties, the flood caused significant damage to the city's infrastructure. The force of the wave was strong enough to lift a piece of the tank and crash it into the nearby railway station. Many blocks were flooded, and some buildings were completely destroyed. It is reported that several factors could have contributed to the disaster [2].

Figure 1: The molasses tank.

Retrieved from: https://csengineermag.com/the-great-boston-molasses-tank-failure-of-1919/

The tank's design was flawed, as the steel used was not thick enough to handle the increasing pressure. The internal pressure rose due to fermentation inside the tank, which increased the levels of carbon dioxide. Additionally, thermal shock, which is defined as fluctuations in temperature, could cause stress in materials, particularly brittle ones. On the day prior to the accident, the temperature had risen from -17°C to 5°C, putting further strain on the already weakened tank. A 2014 analysis revealed the metallurgical reasons for the failure. The steel lacked carbon and manganese, making it brittle when cooled below 13°C. The operating conditions at the time of the failure were 4°C, which was significantly lower than the transition temperature. Another cause of the failure was the presence of fatigue cracks that had developed around a critical point. The tank had been filled multiple times, which subjected the panels to intermittent cyclic loads. These factors, along with the lack of structural assessments (such as inspections and ignoring warning signs like groaning noises), led to the catastrophe [3].

Figure 2: The aftermath of molasses flood.

Retrieved from: https://www.bostonglobe.com/magazine/2019/01/09/the-great-molasses-flood-was-boston-strangest-disaster/VawySumFUf5vKCibM9PLtJ/story.html

2.2.2 Hasselt Bridge

Hasselt Bridge was used to connect the two banks of the Albert Canal in Belgium. The 75m structure was built in order to serve the daily needs for transportation by vehicles and rarely by railway. On March 14th of 1938 the bridge collapsed under a significant initial crack at the lower chord of the structure which had led to excessive loadings at the upper chord resulting in total destruction. No victims had been reported after this accident. The welded construction was made up of aligned arched upper chords and horizontal lower chords that were connected by vertical welded girders. The material that was utilized for building the bridge was Belgium steel St-42.

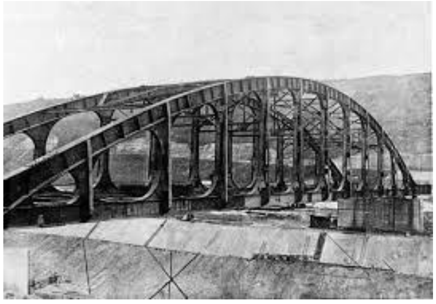

(a)

(b)

Figure 3: (a) The Hasselt Bridge, (b) The bridge after the failure

Retrieved from: (a) https://onlinelibrary.wiley.com/doi/abs/10.1002/stco.201210029 , (b) https://www.researchgate.net/figure/Hasselt-Bridge-after-its-failure-in-March-1938-Source-LOssature-Metallique-1938_fig1_264487722

Despite the fact that the bridge had an adequate resistance to tension the chemical composition of the steel made the structure susceptible to brittle fracture. It had been found that the steel had plenty of sulphur and phosphorus, a fact that indicated the reduced magnitude of toughness which consequently resulted in inappropriate transition temperature. The temperature was -20ºC at the moment of the incident.

Besides that, the welding quality at the failed segment of the bridge was poor. The welding that functioned as a linkage between the flanges of vertical girders and the lower chord’s ones was deficient, meanwhile the residual stresses at this point were extremely high. Hence, the low toughness in conjunction with extremely low temperatures, the inferior welding in combination with the high stress concentration as well as the existence of imperfections caused this disastrous collapse [4].

2.2.3 The Aloha Airlines flight 243

Aloha Airlines flight 243 was a scheduled flight between Hilo and Honolulu in Hawaii, operated using a Boeing 737-297. The plane experienced extensive damage during an uncontrolled decompression of the cabin, but surprisingly landed safely with only one fatality and a few injured passengers. An investigation later determined that the accident was caused by a combination of factors. The airline's maintenance and inspection program were found to be lacking, as fuselage inspections were only performed at night, making it difficult to detect any flaws. The fatigue cracking originated from the knife edge connected to the countersunk rivet holes, which transferred concentrated stresses along the rivets due to geometric discontinuity and lap joint disbonding. The fuselage failure mechanism occurred as a result of several instances of site fatigue cracking near the rivet holes, which diminished the safety factor of the fuselage. It is important to note that the incident occurred after 19 years of service, although the ideal design life was 20 years. This highlights the importance of fatigue prevention, which prompted changes in aviation safety standards and procedures [5].

Figure 4: The plane after the accident.

Retrieved from: https://www.flightsafetyaustralia.com/2016/04/explosive-decompression-of-flight-243/

2.3. Failure Theories

Failure theories play a crucial role in engineering design and analysis. They offer a systematic approach to comprehending the behavior of materials when exposed to various loads. Additionally, they have the ability to anticipate the conditions under which a structure or machine component could fail due to the presence of non-standard loads. Furthermore, they determine safety factors, ensuring safety and reliability. Depending on the behavior of the material (ductile or brittle), different static failure theories are employed. In ductile materials, stresses are evaluated in relation to yield strength, while in brittle materials, they are associated with the ultimate stress strength [6].

2.3.1 Ductile Materials

Ductility is a mechanical property that generally defines a material's ability to withstand plastic deformation without breaking. The tensile test produces a stress-strain curve, which illustrates some physical properties of a ductile material. As shown in Figure 5, the region until stress reaches the yield stress point is the elastic region, where the material can be deformed, but when the load is removed, it returns to its original configuration. The yield strength (σ_y) is defined as the stress at which a constant deformation occurs, and above it, the plastic region begins. Between the yield strength and the ultimate strength, the material resists plastic, permanent deformation through the strain hardening mechanism. Work or strain hardening is an endogenous mechanism that increases the number of dislocations to prevent further deformation. The ultimate tensile strength (σ_{uts}) is the stress at the highest point of the curve and characterizes the maximum resistance to fracture, with the onset of necking appearing. The escalation of stress after necking leads to final fracture.

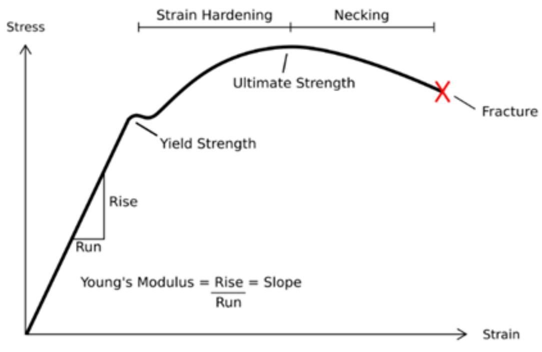

Figure 5: Stress-strain curve for ductile materials

Retrieved from: https://commons.wikimedia.org/wiki/File:Stress_Strain_Ductile_Material.png

The ability of a material to be stretched is determined by two factors. The percent elongation which is defined as:

$\varepsilon = \frac{L-L_0}{L_0} x100$ where,

- L is the final gage length (when it breaks)
- L_0 is the initial gage length

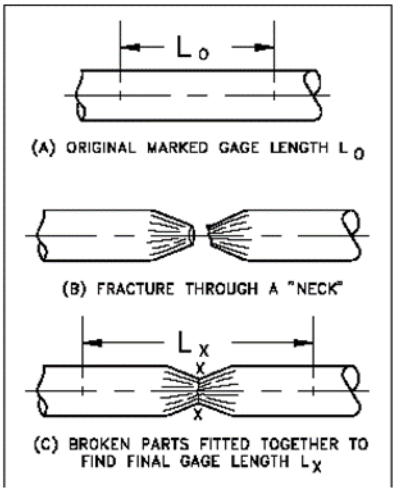

Figure 6: Measuring the elongation after fracture.

Retrieved from: https://www.engineersedge.com/material_science/ductility.htm

The other and more accurate factor is the percent of reduction area which is measured in the minimum diameter of the neck and can be defined as:

$\frac{A_0 - A_f}{A_0} x100$ where,

- A_0 is the area of original cross section
- A_f is the minimum final area [7]

Ductile materials are limited by their shear strength. Static failure theories, that are better indicate the level do the stresses need to reach for fail, are Tresca and Von Mises criteria. The Maximum distortion energy theory or as widely referred ‘Von Mises’ criterion it is broadly considered as the most reliable reference point for design. The method assumes that failure occurs when an effective stress reaches the value of yielding strength in the tensile test. So, it is proved that using Cartesian coordinate system in three-dimensional stress, the Von Mises criterion can be written as,

$$\sigma_e = \frac{1}{\sqrt{2}}[(\sigma_{xx} - \sigma_{yy})^2 + (\sigma_{yy} - \sigma_{zz})^2 + (\sigma_{zz} - \sigma_{xx})^2 + 6(\tau_{xy}{}^2 + \tau_{yz}{}^2 + \tau_{xz}{}^2)]^{1/2}$$

The safety factor is formed as $n = \frac{\sigma_y}{\sigma_e}$ >1 to prevent failure [8]. For the estimation of the shear yield strength, it is considered a state of pure shear τ_{xy} . Thus, using normal yielding stress,

$\tau_{xy} = \frac{\sigma_y}{\sqrt{3}} = 0.577\sigma_y$ which can be noted as $\sigma_{sy} = 0.577\sigma_y$ [9].

The maximum shear stress theory, also known as Tresca criterion specifies the maximum shear stress τ_{max} which led to failure when it becomes equal or exceed to a critical value τ_y i.e., the shear yield strength in a simple tension test specimen of the material. As $\sigma_1 \geq \sigma_2 \geq \sigma_3$ are three principal stresses in descending order τ_{max} can formed as $\tau_{max} = \frac{\sigma_1 - \sigma_3}{2}$ while the τ_y can be written as $\tau_y = \frac{\sigma_y}{2}$ in uniaxial tension where $\sigma_3 = 0 \; and \; \sigma_1 = \sigma_y$. Consequently, the shear yield strength is $\tau_y = \sigma_{sy} = 0.5\sigma_y$. The safety factor is determined as n=$\frac{\sigma_{sy}}{\tau_{max}}$ >1 to prevent failure. The Tresca theory is more conservative but less accurate predictor of failure [10].

2.3.2 Brittle Materials

Brittleness, in contrast to ductility, is the material behavior that describes its inability to undergo plastic deformation. In this case, cracks grow and spread rapidly, causing rapid fracture without prior indication. During a tensile test, the specimen breaks without noticeable yielding, lacking toughness due to insufficient absorbed energy, as shown in Figure 7 [11]. As demonstrated, the ultimate strength coincides with the stress required for failure.

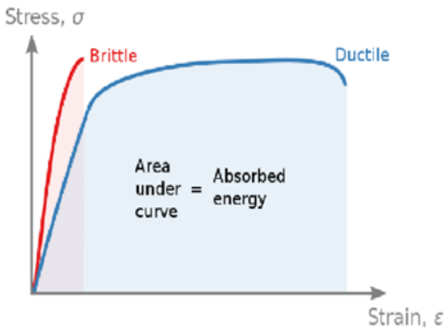

Figure 7: Stress-strain curve for brittle-ductile material.

Retrieved from: https://commons.wikimedia.org/wiki/File:Stress_strain_comparison_brittle_ductile.svg

Thus, brittle materials are limited by tensile strength but can endure high compressive stresses, as their σ_{uts} takes a higher value than in tension, as plotted in Figure 8. This is a result of the presence of blemishes, which weaken the material state in tension but do not affect its resistance to compressive response [12].

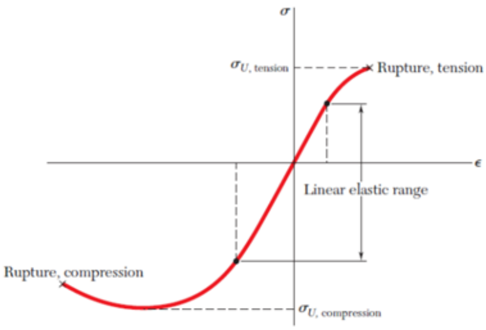

Figure 8: Stress-strain curve for brittle material.

Retrieved from: Mechanics of Materials 7th edition, Beer et al, pp79/901

The Maximum Normal Stress theory assumes that failure occurs when the maximum principal stress σ_1 reaches and exceeds the ultimate strength σ_{uts}. This criterion requires that the σ_{uts} would have the same value in tension and compression, however this assumption is not acceptable in all instances.

Hence, the theory predicts failure for $\sigma_1 \geq \sigma_{uts}$ and safety factor n= $\frac{\sigma_{uts}}{\sigma_1}$ [13]. The maximum principal stress could be calculated by Mohr's circle. It is proved that the center and the radius of the circle are given by

KM=$\frac{\sigma_{11}+\sigma_{22}}{2}$, R=$\sqrt{(\frac{\sigma_{11}-\sigma_{22}}{2})^2 + {\sigma_{12}}^2}$ so the maximum and minimum principal stresses are: $\sigma_1 = \sigma_{max} = KM + R$, $\sigma_2 = \sigma_{min} = KM - R$.

Fracture Mechanics offers a different approach to preventing failure. It is based on the estimation of the stress intensity factor K, which depends on the length of the crack and the applied loads. The value of K is compared with a critical value, K_{IC}, which is the fracture toughness or critical stress intensity factor. The main idea of this theory is to ensure structural integrity by calculating the allowable stresses and cracks. Fracture

Mechanics is a crucial aspect of brittle rupture and will be explained in a following chapter.

3. Marine Structures

Marine structures are classified into ships and offshore platforms, but the term encompasses various disciplines of marine technology, responsible for designing and constructing various structures in the marine environment, including but not limited to ships, platforms, port facilities, submarines, tidal energy systems, and other structures that support human economic activities. These structures are designed to operate in a harsh environment, which includes waves, winds, corrosion, and temperature fluctuations. The main objective of these constructions is two-fold: on one hand, to harness energy sources, such as oil reservoirs in the case of oil rigs, and on the other hand, to maintain the integrity of the supply chain by transporting goods via vessels. [14].

3.1 The Ship

The earliest evidence of boats dates back to Ancient Egypt around 4000 AD. These boats were made of bundled papyrus reeds and had both oars and sails. They were used to meet the trading needs along the Nile River, which was a well-known navigational area. In 2000 AD, the Middle Eastern civilization began venturing into the Mediterranean, so they started making wooden boats to withstand the harsh sea conditions [15]. Centuries later, the Phoenicians made sail crafts for trade and warfare, powered by oarsmen. They introduced famous shipbuilding techniques such as the design of the keel, the technology of the cutwater, which was the ancestor of today's bulbous bow, and the method of caulking between wooden boards [16]. During the Viking Age, longships were made for transportation, exploration, and combat. These vessels had the capacity to hold up to 60 men and could travel across the ocean [17]. In 1000 AD, the Chinese invented the rudder, which is still used to steer ships today and simplify navigation. From 1450 onwards, ships were mostly made of wood and typically had three or more masts. They were used for exploring the world, as battleships in warfare, or for trading. In the mid-18th century, the first steamships appeared, using a combination of steam and wind power to move and make transatlantic voyages. Since the early 19th century, ships have been propelled by diesel engines, which generate the necessary thrust for movement [18].

Vessels are classified as merchant, special purpose, or naval depending on their specific requirements. Each type of ship is further divided into categories based on their function, which involves modifying the primary structural components as prescribed by naval architecture rules. Merchant ships are used to transport cargo and passengers and include oil tankers, LNG carriers, bulk carriers, general cargo ships, container ships, and passenger ships. Special purpose vessels are used for specific operations such as scientific research, offshore supplying, cable laying, and other unique activities. Examples of this type of ship include research vessels, offshore supply vessels (OSV), ocean weather ships, and cable layers. The navy is a component of a nation's armed forces primarily formed for military operations and has the responsibility of projecting military strength through naval vessels such as frigates, aircraft carriers, submarines, and other supporting warships [19].

A ship is a large seagoing vessel that travels by its own means of propulsion, such as an engine or sails. The definition of a ship has changed over the years due to technological advancements. In the past, it referred to a vessel with three or more masts, but today it implies a vessel of over 500 tons of displacement. The primary purpose of building ships is to carry passengers or goods around the world, although they can also serve military purposes. Ships have a specialized crew for the bridge and engine, responsible for navigating the ship safely and operating and maintaining the equipment during voyages.

The lifecycle of a ship, which can last over 25 years, starts with its design. Naval architects lead a multi-disciplinary project as the construction of a ship requires a wide range of engineering specialties. The final design must merge the requirements of each technical field and take into consideration factors such as the route and environment, type of cargo, amount to be transported, value of the cargo, and port amenities. The owner's requests also play a crucial role in the design as they operate the ship to make a profit. The design then evolves into an economical model.

The next step is to create feasible designs, including the machinery, hull structure, and various systems such as electrical and hydraulic. Before construction begins, building and operating costs, as well as the profits and economic evaluation of alternatives, are assessed in an economic report [20]. The entire process is shown in Figure 9.

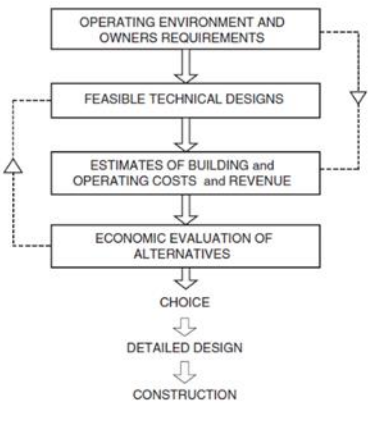

Figure 9: The total flow way.

Retrieved from: The Maritime Engineering Reference Book [20]

Shipbuilding is the production of ships and other buoyant vessels that takes place in specialized facilities known as shipyards. The latest shipbuilding method is block construction, which involves the assembly of prefabricated components that are transferred to the building dock or slipway in a pre-built condition. The components are then joined, and the process continues until the ship is completed.

The shipbuilding techniques have evolved over the years. Before the 1940s, ships were built entirely of welded steel. However, the first welded steel ships used steel with insufficient resistance to brittle fracture, which resulted in dangerous structural cracks (as seen in the case of Liberty Ships) [21].

In 1990, the Oil Pollution Act (OPA90) was enacted by the U.S. Congress to prevent oil spills during accidents like the Exxon Valdez. This law required that all oil ships operating in the U.S. be constructed with a double hull for added safety. The double hull design consists of two water-resistant layers, with the outer hull shaping the ship and the inner layer providing an additional wall to ensure the vessel's integrity and to prevent pollution in the event of a collision. The space between the inner and outer hull is filled with ballast tanks to maintain the ship's stability and prevent pollution in case of an accident. Today, the stainless steel used for ship construction is ASTM A36 standard, which offers a combination of appropriate strength, formability, and ease of welding [22].

Figure 10: Prefabrication process in shipyard.

Retrieved from: http://kalyan-sg.byethost22.com/MPM-II/ShipbuildingCompetitiveness-PaulStott-July2013-02.pdf?i=1

During its working life, a ship requires strong and continuous maintenance and re-equipping processes to keep it in proper condition. Some of these works can be performed by the crew at sea or in port, but many complicated tasks are performed when the ship is in drydock. As shown in Figure 11, a drydock is a structure that allows water to flow in so the vessel can enter the basin, which is then emptied to allow the ship to rest on the dry platform. The main reason for this procedure is to perform effective repairs and maintenance, particularly for parts that are covered by water. These tasks include hull inspection for potential damage, removal of rust, and painting to protect the vessel from the marine environment and corrosion. Additionally, inspections are essential for the machinery, tanks, and cargo spaces. Besides preservation, drydock work benefits the ship's operating status by bringing it closer to its initial design speed and fuel consumption. According to the IMO MARPOL and SOLAS conventions, this procedure must be carried out twice within a five-year period [23].

Figure 11: Drydock in Tuzla,Istanbul.

Retrieved from: My own gallery.

Most modern ships have a lifespan of 25 to 30 years, after which their ability to withstand structural failures is diminished, and charterers' demands for state-of-the-art ships become increasingly rigorous, causing their operating value to depreciate. Ship recycling is the process of disposing of vessels with the primary aim of salvaging useful materials, particularly steel, for reuse. One common technique is ship breaking, which involves the disassembling of an outdated ship's structure for scrapping. Most ship breaking takes place in Asia, where regulations regarding environmental and worker safety and health issues are less stringent compared to those in Europe or the United States. Over 90% of global ship breaking is done along the coasts of Bangladesh, Pakistan, and India [24]. In addition to extracting steel for recycling, workers in the industry are often exposed to hazardous materials that cannot be reused. The global labor union is advocating for improved working conditions in the labor-intensive industry in South Asian countries [25]. In 2013, the European Union introduced a regulatory framework, the EU Ship Recycling Regulation (SRR), which enforces standards in line with the IMO's Hong Kong Convention (HKC), signed in 2004. The HKC aims to ensure that ships are recycled without posing excessive risks to human health, safety, and the environment. The SRR includes a list of 41 shipyards, both inside and outside the EU, where EU-flagged ships can only be recycled [26].

Figure 12: Shipbreaking Yard in Bangladesh.

Retrieved from: https://www.nationalgeographic.com/magazine/article/The-Ship-Breakers

3.2 Offshore Platform

Offshore drilling emerged at the end of the 19th century near southern California. The first structure was a simple wooden pier equipped with a vertical rig capable of drilling the ocean floor. As offshore engineering advanced, the constructions became more complex to prevent corrosion and extend the lifespan of the platform. Reinforced concrete oil rigs were developed in the 1950s to withstand harsh sea conditions. In recent years, up to 12,000 oil platforms made of steel or precast concrete have been built due to continued engineering advancements and increased oil demand [27].

Different types of offshore platforms are designed based on the sea depth, and as a result, there is a range of offshore mooring systems to ensure operational safety. The main purpose of the mooring and anchor system is to keep the platform as stable as possible during its operation. Oil rigs are classified into:

- Fixed platforms are anchored to the seabed, typically in shallow waters, and are supported by legs made of concrete or steel.
- Tension-leg platforms are buoyant structures used in depths ranging from 300 to 1500m. The legs of the platform are anchored to the sea floor to minimize vertical movement.
- Jack-up oil rigs are designed to be self-sufficient, raising their supporting system to the drilling area using a rack and pinion anchor system. Due to the limited length of their legs, they typically operate in depths of up to 150m.
- Floating Production Storage and Offloading (FPSO) is a converted ship that serves as a platform for oil extraction and storage of oil from other production units. FPSOs operate at deep depths, up to 1900m.
- Semi-submersible platforms float using pontoons that are under the ocean surface. These floating platforms are connected to upper facilities by pillars and are secured by large anchors to ensure stability during drilling operations and during severe weather conditions.

Offshore structures are installed in marine environments to carry out energy activities with economic potential. They typically serve multiple purposes, such as generating power through wind turbines exposed to high wind speeds, exporting and transmitting oil and gas through pipelines, and floating solar panels set up on a buoyant craft on a lake. The main objective of developing and constructing offshore structures is to meet the growing demands of the petroleum industry for exploring, drilling, producing, storing, and transporting oil or gas [28].

Oil rigs are large structures equipped with facilities to extract petroleum from reservoirs beneath the ocean floor. Most platforms are self-sufficient for power and water needs, as well as for housing personnel. The average lifespan of a platform is estimated to be 25 years or more while operating in a harsh marine environment. Marine engineers responsible for design and construction projects must draw on knowledge from other scientific fields, including meteorology, geology, naval architecture, ocean engineering, and materials science, to gather geotechnical and marine data. During their operational life, offshore platforms face a hostile environment, especially when located in open seas. Their design must take into account the unique conditions that can cause earthquakes, hurricanes, and high waves, which can lead to structural failures. Oil rigs are made of mild or high-strength steel, although some older platforms were constructed with reinforced concrete. Offshore drilling also has economic implications, as it affects oil prices and is said to reduce unemployment rates and drive economic growth in local communities [29], [30].

The design of an offshore structure is divided into three stages. The first stage involves the layout of the deck that supports the main facilities of the construction, including the drilling deck, production deck, and the lowest floor, the cellar deck, as part of the superstructure.

The second stage pertains to the jacket, a stable lattice structure anchored to the seabed that supports the platform. The placement of the jacket must be selected based on the applied loads such as waves, winds, and water depth.

The third stage involves determining the appropriate strength of the overall construction for launch, installation, and operation procedures. During the design and analysis of oil rigs, several factors must be taken into consideration, including environmental conditions such as the storm history of the location and ground characteristics, as well as building guidelines according to American Institute of Steel Construction (AISC) standards [31].

Figure 13: (a) Offshore Platform, (b) Oil rig jacket.

Retrieved from: (a) https://www.esa.int/ESA_Multimedia/Images/2013/11/Offshore_platform ,(b) https://3dwarehouse.sketchup.com/model/u2a6b3166-5a4a-481a-b454-02420171f85c/Oil-rig-jacket

The design of offshore installations varies based on the type of configuration involved. There are several types of oil rigs used in the industry, but fixed platforms have the most complex installation process due to their separate jacket and topside components. These components are transported to the site using specialized equipment, such as supply boats, which can connect the sections and install the necessary apparatus using welding, bolting, or adhesive bonding if welding is not possible for thin materials. Jackets are lifted from the supply vessel's deck and then lowered to the seabed, as shown in Figure 14. Mudmats, which are horizontal panels made of stiffened steel plate, are placed at the base of the jacket legs to provide resistance to various loads and to withstand the forces during the installation and pile driving process [32].

Figure 14: Installation of an offshore platform.

Retrieved from: https://gr.pinterest.com/pin/installation-of-the-1800tonne-offshore-substation-at-rwo-innogys-48turbine-295mw-nordsee-ost-wind-farm-30km-north-of-the-i--414331234441881726/

The goal of the offshore industry is to achieve high performance by maximizing oil production while minimizing maintenance costs and ensuring safety during inspections. The challenge is to optimize operations and reduce expenses, which are related to the oil price, through regular maintenance checks. Following a preventive approach, identifying potential problems before they escalate, is more cost-effective than fixing issues after they occur. This requires skilled employees with deep knowledge and experience in monitoring equipment status, especially in regard to phenomena such as cavitation and erosion. The expertise of the in-charge engineer in these areas is crucial for maintaining pump systems. Cavitation can negatively impact pumping systems, causing oscillation and hydraulic imbalance, while erosion is a result of high flow velocities and friction from the transfer of sand. Maintaining the functional equipment of oil rigs located in remote areas requires a combination of effective assessment and cost-saving maintenance practices for the turbomachinery system, including pumps, motors, generators, and turbines, that keep the platform operational [33].

Decommissioning is the process of ending oil extraction at an offshore platform and restoring the seabed to its original condition. This process involves a plan in which the oil rig is removed from the site, the wells are sealed, the supporting components, and other operational equipment (such as pipelines) are disposed of, and the platform ends up in a scrap yard or is used for environmental purposes. The cost of decommissioning is high due to the specialized techniques required for dismantling the structure. The topside facilities are cut by welders and diamond-studded saws, and robots are used for disassembling the underwater construction [34].

A more cost-effective alternative is to convert the obsolete platform into an artificial reef, creating a sustainable marine environment. During the flattening of the seabed, which is required for decommissioning, the habitat is destroyed. In contrast, the structure can provide a protected area where an array of species can continue to thrive. The US Congress passed the National Fishing Enhancement Act (NFEA) in 1984, encouraging the fishing community to expand its activities to offshore locations as they provide an ideal marine environment for various interests. It is estimated that the oil industry saves millions of dollars each year by avoiding platform removal and following a reef program, which are invested in further developing the offshore sector (improving safety, maintenance, and production) [35].

The North Sea offshore platforms are leading the way in storing carbon dioxide emissions during natural gas production. The program started in 1996 when Statoil began separating, transporting, and burying the CO2 emissions from its gas field deep under the seabed, with the aim of extending the lifespan of the infrastructure. The project aims to be a shield from rapid climate change by capturing and eliminating carbon emissions, making the 2050 net-zero goal achievable [36].

4. Ductile Fracture

Ductile or cup and cone fracture occurs when a metal experiences significant plastic deformation, causing it to rupture. The permanent deformation begins when the tension exceeds the yield strength σ_y, while the strain hardening mechanism acts as an obstacle to prevent further plasticity. If the process is not interrupted, when the stress reaches the ultimate strength σ_{uts}, which is the maximum resistance to fracture, a neck forms in the material. Once necking begins, the failure process continues with the creation of a triaxial stress state at the midpoint of the material's thickness. Metals or alloys are made up of dispersed second phase particles and inclusions that are affected by the growing action of the stress state, resulting in their rupture and detachment from the matrix material, causing voids to form. As the plastic deformation continues, the triaxial stress causes the nucleation and growth of the voids until the bond between adjacent voids is eliminated, leading to their amalgamation and the creation of an initial crack.

At a microscopic level, voids appear on the fracture surface as small cavities or dimples. The exact shape of these dimples is influenced by the size and structure of the second phase particles or inclusions, as well as the effect of the current loading. The overall appearance of the material gives evidence of the failure mechanism, as evidenced by the rough surface, which suggests plastic deformation and a cup and cone fracture caused by uniaxial tension.

Ductile fracture plays a crucial role in engineering as it provides early warning signs before the final rupture occurs. Ductile materials are capable of undergoing plastic deformation until their limits, as determined by tensile tests. The surface of these materials shows marks that offer a better understanding of the process. Areas that experience plasticity display parallel lines, known as slip bands, which contain a number of microscopic lines called slip lines. The crystalline structure of these materials causes the interaction between the crystalline layers, resulting in the formation of slip bands. This mechanism, triggered by the deformation process, takes place in a specific slip system that involves slip planes and slip directions. However, the crystalline structure also includes imperfections or defects called dislocations. The slip movement of these dislocations within the crystal leads to permanent deformation when subjected to an applied shear stress due to external loading [37].

4.1 Bending

Ships and offshore structures are exposed to harsh weather conditions, which create a hostile environment for their metallic structure. During unfavorable conditions, transverse waves impact the vessel causing vibrations and creaking of the hull. The ship's bow submerges into the sea, then emerges to the surface, while the massive structure balances on the peak of a wave or rolls through valleys. The problem associated with the ship's strain is perhaps one of the most challenging and perplexing among other mechanics of structures issues in terms of loading determination and the structure's response. Like other complex problems, it is crucial to identify a sequence of independent issues and address them individually. For example, smaller parts of the structure such as plating panels and single stiffeners are supported by stiff compounds and are subjected to vertical and horizontal loads. The impact of these forces enables the evaluation of the material's behavior under bending and buckling. Eventually, the entire structure, consisting of decks, bulkheads, and grillages, can be considered as a beam to determine the exact behavior of the ship.

Disregarding the inertial forces caused by the vessel's motion, two main components affect the ship: gravity and hydrostatic pressure. These two loadings cannot cancel each other out at calm waters, let alone during heaving when the loadings change constantly. This results in a lack of stress uniformity along the ship structure, causing her to bend as she is an elastic construction, meaning she can be considered as a floating elastic beam according to the principles of mechanics of materials.

At still water, gravity and hydrostatic pressure act on the ship as two vertical forces, weight and buoyancy. When the decks of the structure are under tension, i.e., the ship is bent with her bow and stern curving downward, the vessel's condition is known as hogging. On the other hand, sagging occurs when the ship is under compression loadings with her edges curved upwards. Hogging and sagging are crucial factors to consider during loading and unloading processes, especially in cargo ships, which can break down if these two states are not taken into account by the chief officer responsible for ensuring the structure's integrity.

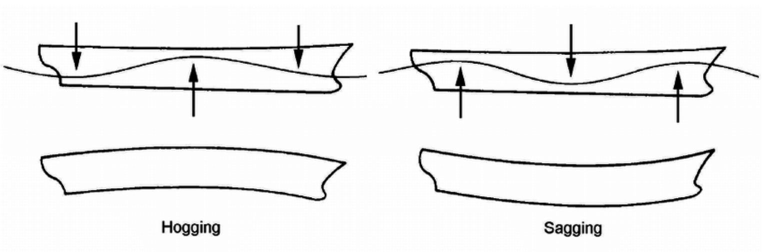

Figure 15: Hogging and sagging condition of a ship.

Retrieved from: https://www.researchgate.net/figure/Hogging-and-sagging-of-ship-hull_fig2_228891097

The hog or sag of a ship is caused by wavy seas. When the center of the vessel is on a lengthy wave peak, the force applied in the middle of the ship increases compared to her edges, causing hogging. On the other hand, sagging influences the hull when there is a trough in the middle and crests at its ends. Overall, in a static situation, the hull is subjected to:

- Loadings that result from the differing longitudinal distribution of the weight and buoyancy forces
- Additional loadings on account of the passing through blocks of waves [38]

4.2 Briefing view of Beam Theory

A beam is considered to be a structural prismatic rod with a length much greater than its crosswise dimensions and is subjected to bending. The lengthwise or simple axis of the beam is assumed to be the geometric location of the center of its cross sections.

When a beam is loaded by forces or force pairs, it creates stresses and twists in its structure. To determine these twists and stresses, we first have to evaluate the internal forces and torques that are applied to the beam's cross section. If a fixed beam is loaded by an external force P at its free end and cut at a section "mn" located a distance x from the free end, this part of the beam is separated to form a free body. At this point, the distribution of the stresses is still unknown, but the result of the applied stress must ensure that the free body is in an equilibrium state.

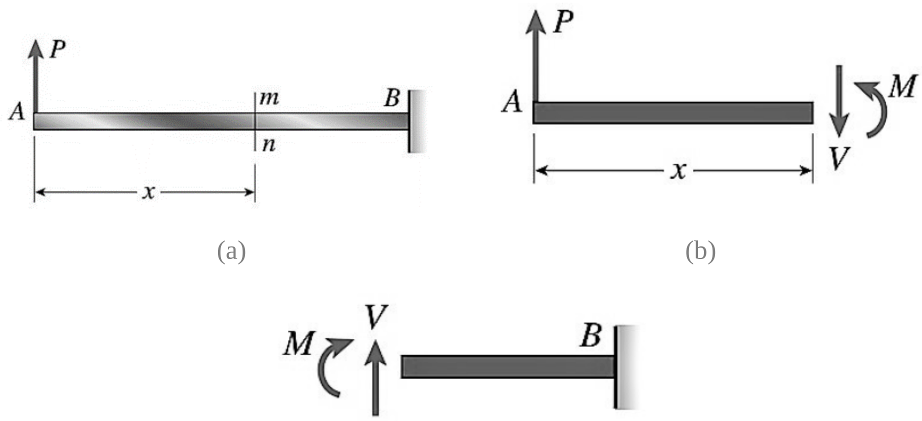

(c)

Figure 16: (a) Cutting m-n, (b) and (c) shear force V and bending torque M.

Retrieved from: [39]

The result of the stress applied at the cross section of the beam can be represented as a shear force V, which generates shear stress, and a bending torque M that creates normal stress. Since the force P is vertical, there is no axial force at the cross section. The shear force, bending torque, axial force, and internal forces are the consequences of the stresses that are distributed at the cross section, and can therefore be calculated using equilibrium equations.

When examining a small part of the beam with a distance of dx between two cross sections, it is important to develop equations that connect the aforementioned forces to form shear force and bending moment diagrams throughout the length of the beam. The load applied on the upper surface of the elementary part dx can either be a distributed load or a concentrated load.

If we consider a distributed load, the increases in shear force V and bending torque M are infinitesimal and are represented as dV and dM, respectively. The corresponding resultant forces on the right side of the part are $V + dV$ and $M + dM$. The difference between a distributed load and a concentrated load is that under a concentrated load, the values of M and V can be finite.

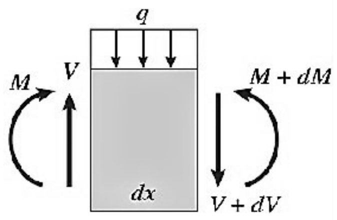

Figure 17: The elementary part dx and the distribution of the forces and torques.

Retrieved from: [39]

Hence, regardless of the type of loading, there are two equilibrium equations that spring from the assumption of equilibrium conditions: the equilibrium equation for the vertical forces and the equilibrium equation for the torques.

From the first equation a relation between the distributed load q and the force is obtained:

$$\sum F_y = 0$$

$$V - qdx - (V + dV) = 0$$

So, it results to $\frac{dV}{dx} = -q$

The second equation provides the relation between the shear force and the bending torque,

$$\sum M = 0$$

$$-M - qdx\frac{dx}{2} - (V + dV)dx + M + dM = 0$$

Thus, $\frac{dM}{dx} = V$

The expression that connects the tensile or compressive stresses with the lengthwise bending according to the theory of elastic bending is written as,

$$\sigma_x = -\frac{M}{I}y$$

Where,

- σ_x is the flexural stress
- I is the moment of inertia
- y is the distance from the neutral surface [39]

It has been verified that the stress is compressive ($\sigma_x < 0$) above the neutral axis ($y > 0$) when M has positive value and tensile ($\sigma_x > 0$) when it has negative values.

The expression for σ_x not only determines the maximum stress, but also the stresses at every point along the cross-section. To specify the exact point and value of the maximum bending torque, diagrams are necessary. The bending moment diagram helps in determining the M at different points along the beam, which is designed based on the distance x calculated from one end of the beam. A corresponding shear diagram, referring to the shear force V, is also formed.

The shear stress indicates the presence of a vertical shear force Q applied at the cross-section of the beam. For an elementary dx, Q causes a change in the bending moment, resulting in $dM = Qdx$. This adjustment causes the normal stresses to differ at each side of dx.

The equilibrium equation for the horizontal direction is written as,

$$\sum F_x = 0$$

$$\tau t dx + \int_0^s (\sigma_D - \sigma_C)\, t\, ds = 0$$

Where,

- $\sigma = \frac{M}{I}$

Then, $$\tau t dx = \frac{M_D - M_c}{I} \int_0^s y t ds$$

Thus, combing the above-mentioned expressions, shear stress can be stated as,

$$\tau = \frac{Qk}{It}$$

Where,

- t is the element amplitude at the cut.
- Q is the static torque from the neutral axis of the crosswise cross section part
- $k(s) = \int_0^s y t ds$, k is a function of the rib's geometry

The product of τ and t is called shear flow, q, which is a significant magnitude because of its ability to describe the shear stress caused by crosswise loadings [12]. The following table illustrates the distribution of bending moments and shear forces under different loading conditions.

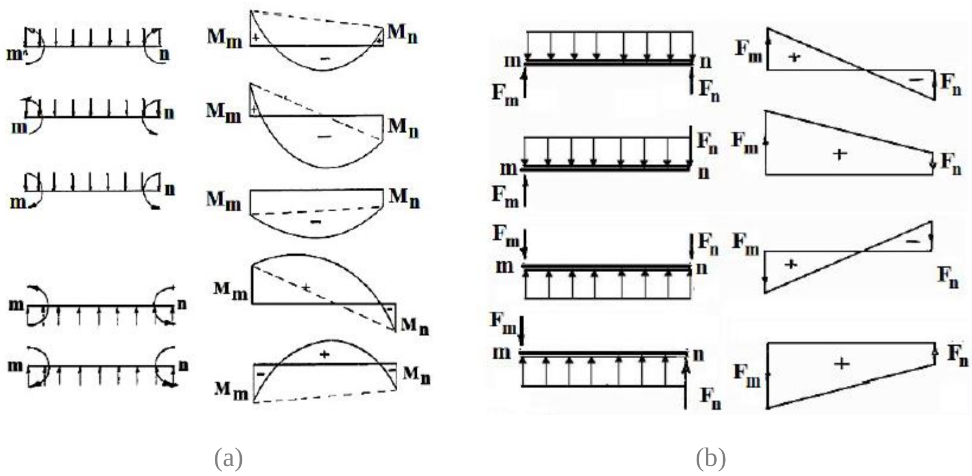

Figure 18: (a) Bending moment distribution for various conditions, (b) Shear forces distribution for several loading conditions.

Retrieved from: [40]

4.3 Ship-girder

The ship is considered a girder in which both static and dynamic loads are applied. These factors are of major significance as they are associated with bending moments and shear forces. The bending moments arise from the differences in weight distribution, such as the weight of the ship and its cargo, along the ship's construction and the buoyancy forces along the length of the ship. Dynamic loads include wave-induced hydrodynamic forces, impact loads, and motion-related inertia loads. These dynamic wave loads result in torsional and bending moments, as well as horizontal and vertical shear forces.

In still waters, the lengthwise strength of a ship is treated as a non-uniform beam that is affected by the distribution of loads across its structure. This load can be determined by the difference between the downward weight load and the upward buoyancy forces. Equilibrium conditions require a balance between the total weight loads and mass acceleration and the overall buoyancy forces and hydrodynamic reactions.

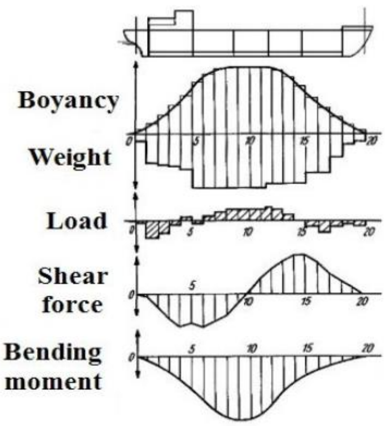

Figure 19: The distribution of the loading, bending moment and shear force along the ship in still waters conditions.

Retrieved from: [40]

The waves impact the bending moments and shear forces due to the alteration they bring to the ship's still-water condition. The ocean waves result in a different distribution of forces as they move past the ship's hull. This varying distribution stems from the unique characteristics of the waves, the speed of the ship, the draft, the trim, and the ship's heading in relation to the waves. If considered a crest at the center of the ship's hull and a wave that is the same length as the ship, the bending moments and shear forces can be calculated as follows.

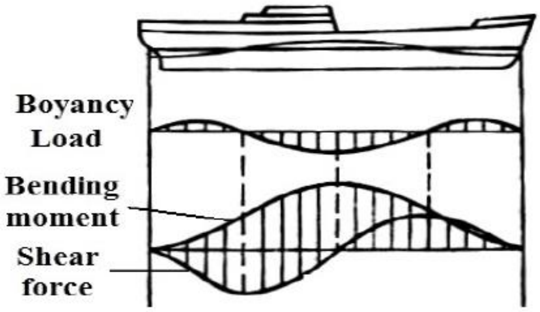

Figure 20: Bending moment and shear force contribution caused by wave.

Retrieved from: [40]

The ship can be in an inclined position due to weather conditions or the varying distribution of its cargo. Under these circumstances, one of the upper decks and its counterpart at the bottom will encounter high bending stresses, estimated by the expression,

$$\sigma = \frac{Mcos\theta}{I_x} y + \frac{Msin\theta}{I_y} x$$

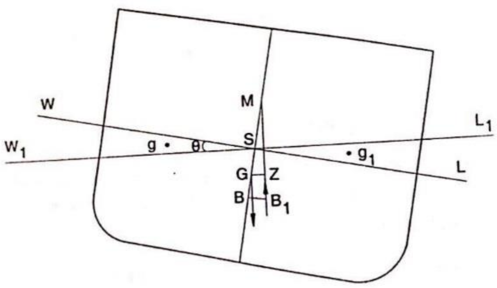

Figure 21: The ship in the inclined condition.

Retrieved from: https://knowledgeofsea.com/transverse-stability/

Shear forces result from the distribution of weight loading across the ship, but they can also be induced (the horizontal component) due to wave action when the ship travels at an angled direction compared to the wave direction. The total vertical shear force can be expressed as,

$$V_V = V_S + V_W + V_d$$

Where,

- V_S the vertical shear force at still-water conditions
- V_W the vertical wave component
- V_d dynamic component

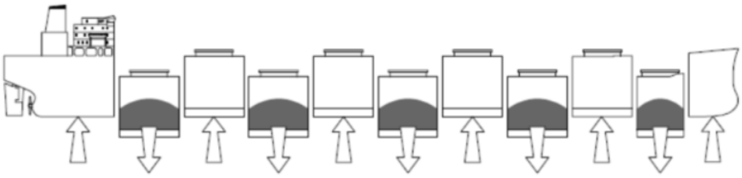

Figure 22: Shearing action of the hull girder in still water.

Retrieved from: https://www.theshipyardblog.com/modes-of-failure-in-bulk-carriers/

The shear force applied at any point along the ship is the force that tries to move one part of the ship vertically relative to the other. The maximum magnitude appears at the neutral axis, at points where the shear force has the greatest rate. Shear stresses can cause failure through warping of the plates in the crosswise direction. Calculating these stresses provides useful information about the suitability of the thickness of the plates and the distance between the plates used to reinforce the structure.

It is important to note that the above-mentioned analysis for the estimation of lengthwise bending moments and vertical shear forces is based on the idealized ship (girder) behavior, without taking into account the impacts of local loading. This is especially relevant for bulk carriers, as the possibility of an unequal distribution of cargo in their holds can affect the results.

Torsion loading is a crucial factor that greatly impacts a ship's behavior during its voyage. The twisting forces generated by waves are a result of the ship's movement being angled compared to the direction of the waves. The waves create torsion, causing the ship's hull to twist along its length, resulting in intense rolling motions and substantial dynamic stresses and torque. When the ship sails diagonally, there is a decrease in bending moments, but an increase in horizontal and twisting moments. The presence of hydrostatic and hydrodynamic forces, along with the forces generated by the ship's movements, contribute to the formation of torsional moments.

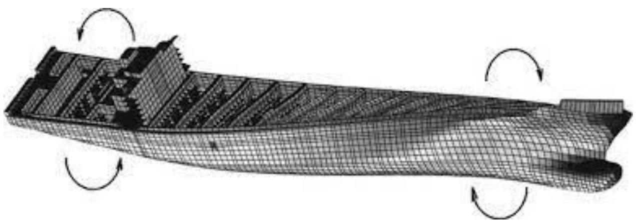

Figure 23: Torsional deformation of a hull girder.

Retrieved from: https://link.springer.com/chapter/10.1007/978-3-642-14633-6_4

4.4 Briefing view of Buckling

The stability of a structure refers to its ability to resist applied loads without undergoing a sudden change in its dimensions. Minor faults and imperfections that result in slight deviations from the designed operating conditions are considered stable. Buckling is a mode of failure that affects ship components under compressive loads and is caused by deviations from the idealized design of columns under stress. The lowest buckling capacity, or critical buckling load, represents the buckling mode of a column. To ensure the safety of the mission, the stability of the entire structure and its components must be maintained. However, real columns may fail under a lesser load due to unavoidable geometric discontinuities and small flaws.

When a straight rod is subjected to a compressive load P, it will initially remain straight. Upon removal of the load, it will return to its original condition. If an increased load P is applied until the work done is equal to the work done by bending, the load P will reach its critical value. At this state, the shape of the rod changes, becoming curved and transitioning to an unstable state. If the load is applied eccentrically or if the rod has a slight curve before the load is applied, the rod will briefly deform after the load is applied.

The critical force is expressed from Euler's formula as,

$$P_{cr} = \frac{\pi^2 EI}{L_e^2}$$

Where,

- I is the area moment of inertia
- L_e is the reduced or the effective length of the column

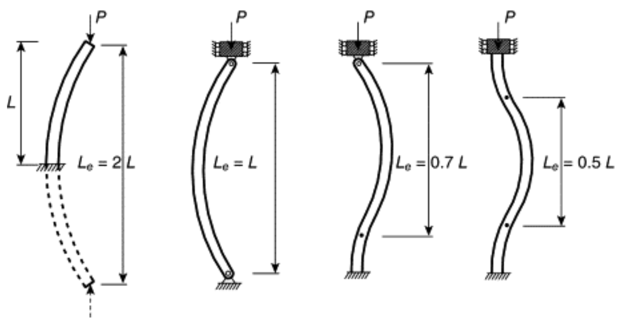

Figure 24: Effective length of column for various end conditions.

Retrieved from: https://www.sciencedirect.com/science/article/pii/B9780857092342500178

The effective length is the length at which a rod with hinged ends has the same stability as a rod with specified end conditions.

This equation indicates that buckling occurs under the yield stress σ_y, therefore the critical value of the force P is dependent on the modulus of elasticity E, not on its strength. If $P < P_{cr}$, the solution is considered stable.

The buckling stress is written as,

$$\sigma_{cr} = \frac{P_{cr}}{A} = \frac{\pi^2 E}{(L/r)^2}$$

Where,

- $I = Ar^2$
- $\lambda = \frac{L}{r}$, the slenderness ratio

Buckling is a common phenomenon that occurs in stiffened panels, which are a basic component in ship construction. In deck structures that are strengthened lengthwise, the longitudinal beams serve as stiffeners, and the massive transverse girders are the transverses. In deck structures that are strengthened transversely, the deck beams are the stiffeners, and the hefty deck transverses are the girders.

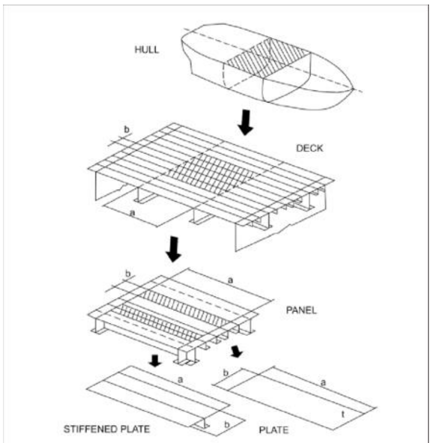

(a)

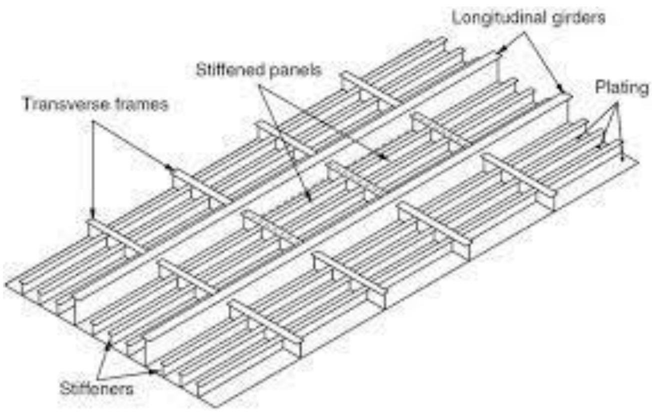

(b)

Figure 25: (a) Thin-walled stiffened structure, (b) The stiffened plates.

Retrieved from: (a) https://www.researchgate.net/figure/Ship-hull-girder-as-a-box-like-thin-walled-stiffened-structure_fig1_237036470 , (b) https://ntnuopen.ntnu.no/ntnu-xmlui/bitstream/handle/11250/2488454/stiffened%2Bpanel.pdf?sequence=2&isAllowed=y

According to Euler's formula the strength expression for a plate panel is given as,

$$\sigma_E = \frac{k\pi^2 E}{12(1-\upsilon^2)}(\frac{t}{b})^2,$$

Where,

- σ_E is the buckling stress
- b is the length of the smaller width of the plate
- a is the length of the larger width of the plate
- t is the plate thickness
- υ is the Possion's ratio
- k is a coefficient that is based on the geometry, boundary conditions and loading distribution.

Buckling can cause significant damage to ship structures, leading to catastrophic results. Therefore, there is a critical value that ensures the ship will not break. The critical buckling limit state for a transversely stiffened deck structure is expressed as:

$$M_f < M_{cr}$$

Where,

- M_f sagging yield point at deck
- M_{cr} the buckling critical value of deck plating

(a)

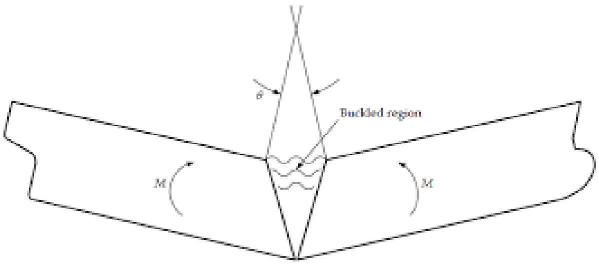

(b)

Figure 26: (a) M/T Prestige, (b) Yielding of deck structure of a ship hull girder.

Retrieved from: (a) https://safety4sea.com/cm-learn-from-the-past-prestige-sinking-one-of-the-worst-oil-spills-in-europe/ and (b) https://ocw.snu.ac.kr/sites/default/files/NOTE/Lecture%2009%20Ultimate%20Strength%20of%20Ship%20Hulls.pdf

The members of a ship subjected to compressive loads, such as girders, longitudinals, and plates, should have adequate buckling strength to prevent the failure of the ship. When the ship is in a hogging condition, the bottom members experience buckling, and when it's in a sagging condition, the deck structure exhibits the phenomenon. To evaluate the buckling that affects stiffened plates with compressive loads, it's important to consider major factors, such as:

- Imperfections, flaws, geometrical discontinuities
- Residual stresses from welding processes
- Boundary conditions [40].

5. Brittle Fracture

Brittle fracture is a rare type of fracture that can have detrimental effects on construction and endanger human life. It occurs suddenly, rapidly, and without prior indications. In the past, engineers focused on making materials capable of withstanding plastic deformation by increasing their yield strength, neglecting their toughness, which is responsible for the material's ability to resist loads without breaking under an initial crack. After several destructive accidents involving materials that failed under yield stress, the scientific community shifted its focus to preventing brittle failure.

The breakage of materials is due to two main reasons: pre-existing cracks combined with the mechanical behavior of materials under stress and low toughness. Unlike ductile fracture, brittle fracture has a smooth surface between the separated components, indicating a lack of plasticity. Cracks often result from flaws in a structure, especially during welding, where high temperatures and rapid cooling can lead to the formation of cracks in the heat-affected zone. The propagation of cracks, which typically occurs perpendicular to applied stresses, depends on fatigue and stress-corrosion, two types of failure that contribute to the final rupture.

Toughness plays a crucial role in brittle fracture as it measures the amount of energy absorbed and plastic deformation before failure occurs. It is therefore considered an important factor in the field of fracture mechanics.

Brittle fracture at the microstructure level is mainly formed by two mechanisms:

- Transgranular fracture: This type of rupture occurs when the crack grows along the grains of the material due to cleavage. A polycrystalline metallic solid is composed of many adjacent grains, each with a different direction from the fracture's spreading line. Due to the resistance encountered at grain boundaries, the crack propagates along weaker crystallographic planes, resulting in a polyhedral smooth surface at the grain scale.
- Intergranular fracture: This type of fracture occurs when phenomena such as phase settling and adhesion of separated chemical elements to the grain boundaries reduce their resistance. The crack then travels through the boundaries without affecting the integrity of the grains. Intergranular fracture is often seen in erosion when high temperatures occur and under applied mechanical stresses, which tend to wear out the material [41].

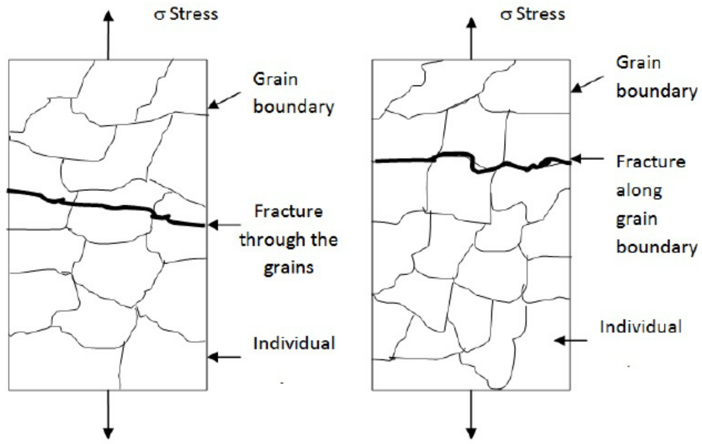

Figure 27: Transgranular (left) and intergranular fracture (right).

Retrieved from: https://yenaengineering.nl/britle-and-ductile-fracture/

5.1 Fractography

Fractography is a method used to analyze fracture surfaces with the aim of understanding the relationship between the microstructure and the causes of crack initiation and propagation, and ultimately the underlying cause of the failure. This study is significant for the field of failure analysis as it provides crucial knowledge and aids in the investigation of a breakage event. The examination of a failed surface can be performed using the naked eye, a magnifying glass, or an electron microscope. However, before testing the surface, it is necessary to clarify several aspects, such as the unique features of each material.

Different materials are expected to have different behavior under the same type of failure, due to factors such as processing, surface quality, brittleness, or ductility. It is important to determine the origin of the failure and conduct a thorough examination for potential defects and locations where concentrated mechanical stresses are applied. The texture of the surface, which distinguishes materials as brittle or ductile, is the primary observation. Ductile materials are characterized by rough fracture surfaces, due to their ability to undergo plastic deformation under high stress, while brittle materials have smooth outer planes due to their inability to withstand mechanical strains. Additionally, during brittle fracture, the surface becomes gradually rougher as the crack velocity increases and ultimately leads to the final fracture.

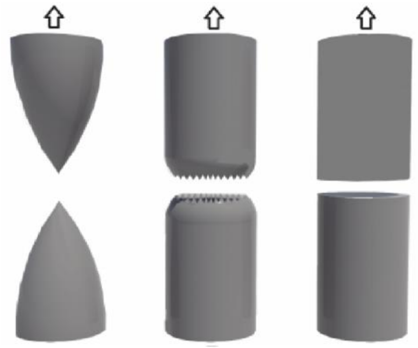

Figure 28: Very ductile materials (left), moderately ductile fracture (middle), brittle fracture (right).

Retrieved from: https://www.researchgate.net/figure/Brittle-vs-Ductile-fracture-a-Very-ductile-soft-metals-eg-Pb-Au-at-room_fig2_221914692

The presence of lines or other markings indicates different failure mechanisms, so it is essential to examine the exact type of fracture using fractography methods such as hackles. The direction of the crack is a major issue, as it indicates the type of fracture. The most common type, Mode I fracture, is characterized by a crack path in the same direction, while in some cases, cracks may follow opposite paths, forming Mode II (in-plane shear) or Mode III (out-of-plane shear) failure, and resulting in a step pattern on the surface. The shape of the crack (linear or curved) provides information about the material's microstructure, the presence of flaws, and the tension applied. The presence or absence of crack branches, which are often caused by impact under high loads, is also an important clue for failure investigation.

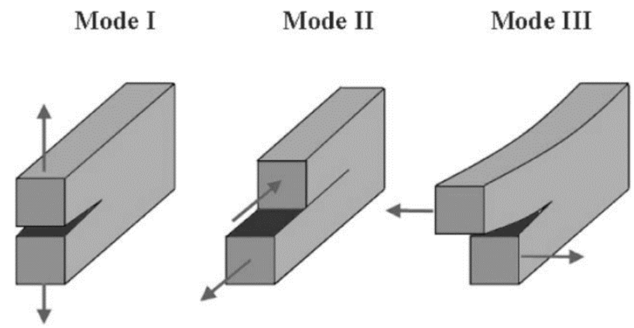

Figure 29: The three modes of fracture.

Retrieved from: https://www.researchgate.net/figure/Three-modes-of-fracture-in-a-cracked-body-Mode-I-is-the-opening-mode-mode-II-is-the_fig3_228799371

Chemical elements from hostile environments can also contribute to fracture, and there are techniques to detect and isolate them, even if they are not visible to the naked eye or under magnification. The contribution of fractography as a failure analysis tool can be summarized into three steps: locating the source of the fracture, defining the crack path, and finally, assessing the type of failure. This knowledge is essential for investigators to reach the root cause of accidents, in combination with environmental considerations and material properties. However, it is important to note that fractography is not the only field that provides information for failure, so it should be incorporated into a comprehensive framework that involves the collaboration of various failure analysis tools [42].

5.2 Impact Test and Ductile to Brittle transition temperature

The Charpy impact test or Charpy V-notch test was developed by Georges Charpy in 1900 to determine the mechanical properties that determine a material's brittle or ductile behavior. The aim of the test is to calculate the energy absorbed by a notched specimen when it breaks from the imposed impact stress. The test equipment consists of a 55mm x 10mm x 10mm notched V-shaped specimen and a hammer that is held on a pendulum arm. The hammer is raised to an initial height and then released to strike the specimen at the opposite site of the notch. After the impact, the final height of the hammer is measured, and the difference between the initial and final heights (dynamic energy) is interpreted as the amount of energy the material can absorb at a specific temperature.

The test results show that materials with high energy can be characterized as ductile, while those with low energy are brittle [43]. Figure 30 illustrates the test outcomes for different metals in relation to temperature.

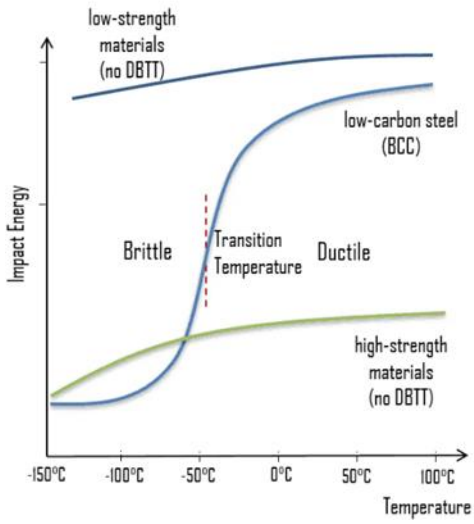

Figure 30: Energy-temperature diagram and ductile to brittle transition temperature.

Retrieved from: https://www.nuclear-power.com/nuclear-engineering/materials-science/material-properties/ductility/ductile-brittle-transition-temperature/

According to the diagram, when the temperature is lowered, notched high-strength materials can undergo brittle fracture even under low stresses in the elastic region due to their inability to absorb impact energy. Low-strength materials such as FCC (such as Cu, Ni), HCP (such as Zn, Mg), and austenitic stainless steels are prone to ductile fracture because of their ability to respond to high energy during tests. These two categories do not show any Ductile-to-Brittle Transition Temperature (DBTT) behavior across a wide range of temperatures. On the other hand, BCC materials, regardless of their strength, exhibit a change in behavior from ductile to brittle due to a range of low temperatures over which the DBTT phenomenon occurs. This is because thermal activation facilitates the movement of dislocations. However, at low temperatures, thermal activation is lower, making it harder for dislocations to move through the crystal due to increased friction. Additionally, the yield stress increases while the plastic zone (the part beyond the fracture zone related to pit formation) decreases, leading to a change in the type of fracture from ductile to brittle.

Since there is no clear standard, the transition temperature is determined as the temperature that corresponds to a specific impact energy (20J) or corresponds to a specific fracture appearance (e.g., 50% ductile fracture). It is important to determine the transition temperature in material design, and it is recommended not to use the material below that temperature as it can lead to detrimental effects on the structure's integrity [44].

Brittle fracture and transition temperature are influenced by notches and metallurgical factors. The former can be linked to fracture toughness, a mechanical property that measures the energy absorbed when creating a unit of fracture surface. This factor describes a material's ability to withstand rupture under an initial crack. Fracture toughness decreases as temperature drops. It is also affected by panel thickness. With thin materials, toughness is highest under plane stress conditions ($\sigma_3 = 0$) but decreases as plane strain conditions impact plastic yielding at the crack edge and material thickness increases. In thick materials, toughness is lowest under plane strain conditions at the crack tip [45].

According to metallurgical factors, steel alloys with adequate toughness can be achieved by reducing carbon content to increase transition temperature, maintaining a Mn:C ratio greater than 3:1, avoiding the use of excessive chemical elements such as P and S, and keeping the Mn:S ratio high. Grain size is also important, as smaller grain size materials tend to reduce transition temperature while increasing ductility [46].

5.3 Fracture Mechanics

The field of Fracture Mechanics is a relatively new sector of engineering, having been developed in the last century after several disastrous accidents highlighted the need for advancing a method to prevent brittle fracture. The production of materials is accompanied by internal and external imperfections that form during processing, but not all of these imperfections result in an unstable state while the material is in use. Fracture mechanics is a critical study that determines the conditions under which a flawed structure can be reliable and predicts the conditions in which a defect evolves into a propagated crack, leading to structural failure.

The method provides an organized approach to avoiding fracture by correlating parameters such as stresses, pre-existing cracks, and fracture toughness. The fundamental theory of the analysis relates the measurement of the localized stress at the crack initiation point, summarized as the stress intensity factor K (which comes with a sign associated with mode I, II, III), to the length of the crack a and the applied stresses. With the configuration factor Y, which depends on specimen features and the type of loading, the factor K for mode I can be written as: $K_I = Y\sigma\sqrt{\pi\alpha}$ (MPa$\sqrt{m}$).Thus, the critical stress intensity factor or fracture toughness for Y=1 is $K_{IC} = \sigma\sqrt{\pi\alpha}$, and when K_I reaches this key value as a result of a combination of a particular σ and a specific crack length α, the crack will grow and lead to rupture [47].

The validity of fracture mechanics relies on the complete absence or minimal presence of plastic deformation prior to fracture, allowing small-scale yielding to be observed. According to Linear Elastic Fracture Mechanics (LEFM), if the plastic zone at the edge of the crack is minor compared to its length, the assumptions of this theory can be applied. In this case, the stress state at the tip of a crack is considered to be close to elastic conditions. Under plane stress conditions, the plastic zone is characterized as a circle with a radius of $r_y = \frac{1}{2\pi}(\frac{K_I}{\sigma_y})^2$, where σ_y is the yielding stress.

Furthermore, LEFM implies that the plastic zone is much smaller in other specimen directions and the material is thick enough under plane strain terms ($\varepsilon_3 = 0$). Therefore, in order to describe the stress state outside the plastic zone and apply LEFM, K_{IC} the following must be applied:

- $r_y = \frac{1}{15}(a, W - a)$, where W is specimen width, α the crack length
- $r_y \leq \frac{1}{15} b$, where b is the specimen thick
- $b \geq 2.5(\frac{K_{IC}}{\sigma_y})^2$

It is important to note that the intensity factor depends on thickness. As the material becomes thinner, the K_I approaches the critical value, K_{IC}. This is why the majority of brittle fractures occur in materials with large thickness. Furthermore, in the case of ductile materials, when the plastic zone becomes larger, K_I is no longer able to accurately define the current conditions, and LEFM is insufficient. In such cases, the theory of Elastic-Plastic Fracture Mechanics (EPFM) is applied by conducting dynamic experiments known as CTOD. The results are interpreted through a fracture parameter, J (J-integral), which extends K_{IC} into the elastic-plastic region.

For design purposes, it is necessary for the intensity factor, K_I, to be lower than the material's toughness, K_{IC}, in order to prevent failure. This is affected by both the loading stress and crack length. The mechanisms that contribute to rapid crack propagation are fatigue and stress corrosion, resulting in a critical length, a_f , that leads to rupture. If the applied stress exceeds a predetermined rate, it can also cause failure. By selecting a material with higher fracture toughness and conducting a damage tolerance analysis, associated with LEFM, the process of crack growth can be monitored and regulated accordingly [48].

6. Corrosion

Corrosion is defined as the interaction of metal with the operating environment and is a type of failure associated with various detrimental structural incidents. The phenomenon progresses gradually, influenced by environmental, metallurgical, and electrochemical conditions. More precisely, corrosion is described as the degradation of metal due to an electrochemical reaction between the metal or alloys and the environment, or the spontaneous conversion of a metallic compound back to its original state. The presence of oxides, moisture, chlorides, acids, and oxygen creates a corrosive environment. As metals are decomposed into their chemical compounds, which have a thermodynamically stable natural state, corrosion is often referred to as reverse metallurgy.

Corrosion occurs when metals are exposed to electrolytes, a high concentration of salt dissolved in soil, and moisture in the atmosphere. This interaction leads to corrosion in liquid, soil, and atmospheric forms. The impact of this mode of failure can be seen on the entire surface of the metal or limited to specific local areas.

Corrosion is an electrochemical phenomenon that involves two simultaneous reactions: the anodic or oxidation reaction, which causes the metal to break down and releases electrons, and the cathodic or reducing reaction, which attracts and consumes the electrons released. The energy difference between these two reactions drives the overall reaction.

Ships, as structures operating at sea, suffer from liquid corrosion, especially the submerged part of the vessel, due to the main form of material they are made of, iron. Iron (Fe) is an electrochemically positive element that tends to release electrons to become a neutral ion. As a result, Fe loses electrons from the exterior surface of the metal, producing positive ions Fe^{2+}. The abundance of dissolving chemical compounds, such as oxygen (O_2) and water (H_2O), in seawater, forms an electrochemically negative hydroxide ion OH^-. This reacts with the positive Fe^{2+} and creates the well-known rust. The steps of the reaction leading to the final product (rust) are written as follows:

$2Fe \rightarrow 2Fe^{2+} + 4e^-$, the anodic reaction

$O_2 + 2H_2O + 4e^- \rightarrow 4OH^-$, the cathodic reaction

Hence, the overall corrosion of iron is,

$2Fe + 2H_2O + O_2 \rightarrow 2Fe(OH)_2$

Rust is formed when the iron oxide, $Fe(OH)_2$ oxidized under the presence of oxygen and water,

$4\,Fe(OH)_2 + 2H_2O + O_2 \rightarrow 4\,Fe(OH)_3$

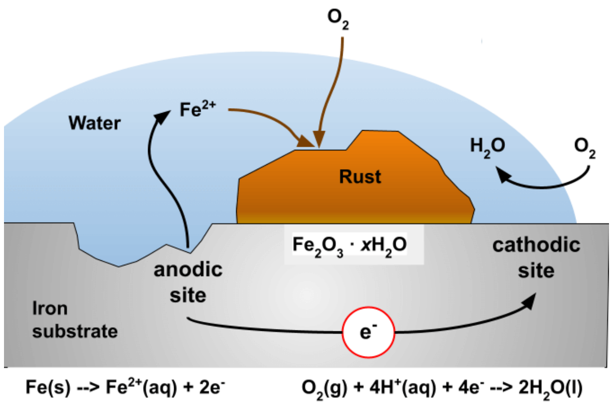

Figure 31: The production of the rust.

Retrieved from: https://www.corrosionpedia.com/8-things-to-know-and-understand-about-iron-corrosion/2/6895

6.1 Passivity and Galvanic Series

A metal with passive corrosion behavior is characterized by a decreasing ratio of anodic disintegration under a constantly increasing applied electrochemical potential, leading to higher cathodic values close to those of noble metals. Passive metals resist further corrosion due to the presence of a passive film, a thin layer that covers the outer surface of the metal. This film prevents further oxidation from occurring, acting as a protective shield, and has the ability to regenerate if damaged. However, passive metals are not invulnerable, as a hostile corrosive environment in which they interact may entail conditions that curb their defensive effect. For example, the presence of chlorides has a destructive impact on stainless steel, and the influence of a low pH solution can transform the passive behavior of the metal to active. Active metals are naturally corroded due to the higher potential of their ions compared to those in the solution where dissolution takes place, leading to a much lower tolerance to corrosion.

The galvanic series is a standard that provides the necessary information for defining and inhibiting corrosion. To determine the galvanic series table, which classifies metals and semi-metals based on their level of nobility, an experiment is conducted. The first step is to create the galvanic cell, namely, to determine a volume of electrolyte (e.g. seawater) and then immerse two disparate metals into it, connecting them with a source of electrical potential. The purpose of this process is to establish the nobility of the metals based on their ability to undergo corrosion. The metal with less noble behavior exhibits corrosion first. Thus, it is extremely important to join the appropriate combination of metallic materials, especially when they are exposed to a corrosive environment such as seawater. The second step is to record these results to form a table that acts as a guideline for optimal selection of collaborating materials. As shown in Fig. 33, the table ranks the metals based on nobility. The higher the noble behavior of a metal, the more cathodic performance it shows. Hence, the table allocates the metals from the most cathodic, unlikely to undergo corrosion, to the most active metals, which are corroded spontaneously [49].

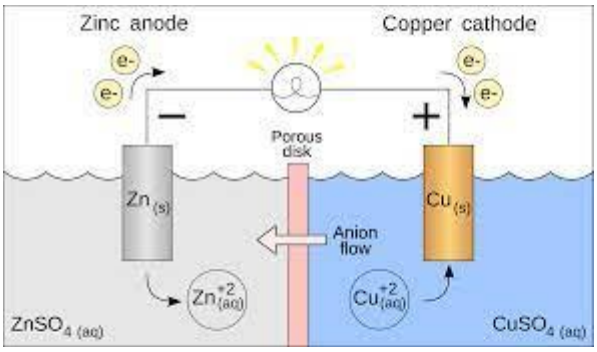

Figure 32: The galvanic cell.

Retrieved from: https://en.wikipedia.org/wiki/Galvanic_cell

Figure 33: The galvanic series table.

Retrieved from: https://www.sciencedirect.com/topics/engineering/galvanic-corrosion

Rust is the primary enemy of the shipping industry, as ships operate in a corrosive environment (atmospheric and aqueous) containing chemical compounds that cause damage not only to the hull of the ship, making it thinner and vulnerable to other modes of failure, but also to her equipment and structural compartments (ballast and cargo tanks, pipes, decks). The cost of addressing and preventing corrosion in the marine industry is estimated at around 80 billion dollars each year, a fact that highlights the significance of this underestimated issue and the importance of resolving such challenging difficulties [50].

6.2 Types of corrosion

Corrosion has been the root cause of a challenging and long-lasting issue: the impairment of marine structures in their functioning environment. It contributes to reducing their life expectancy and also affects their operational status. Some forms of corrosion do not have significant adverse effects, as they can be easily identified and addressed. However, there are certain types of corrosion that can have devastating consequences, putting the integrity of the structures at risk. The most common forms of corrosion found in the marine industry range widely, from general or uniform deterioration of the surface to localized ones affecting specific components.

6.2.1 Uniform

General or uniform corrosion affects a large segment of metal and decreases its thickness due to decomposition. The electrochemical reactions result in the production of rust, which, although more stable than the initial metal, leads to continuous surface deterioration and exposes newly formed metal to a moist environment after disintegration.

Figure 34: The ship's hull affected by uniform corrosion.

Retrieved from: http://www.amteccorrosion.co.uk/m_corrosionresistantship.html

This type of corrosion is the most common in marine structures, resulting from aqueous and atmospheric corrosion in the operating environment of ships and offshore structures. Owing to the fact that is being easily detected and prevented by estimating the lifetime of the phenomenon, uniform corrosion is considered a non-threatening factor to the integrity of the structure.

6.2.2 Pitting

Pitting or localized corrosion is a type of corrosion that accumulates in localized areas on the surface of metal and is identified by the presence of holes and hollow spots (pits) that can penetrate deeply into the material. The severity of pitting corrosion is dependent on the environment, especially if it is aggressive, consisting of chlorides, oxides, and dissolved oxygen. Localized corrosion occurs when a portion of the passive film is damaged by high concentrations of chemical elements, particularly due to the presence of chlorides. It is mainly found at defective or unstable zones of the passive film, such as in the vicinity of welded parts or when the strain hardening process creates an excessively thick oxide film. Moreover, rough surfaces are more prone to pitting compared to smooth surfaces, which resist localized corrosion.

The propagation of pitting is described as a process where the anode is the damaged passive film, and the cathode is the adjacent intact area. As corrosion progresses, metal cations move to the formed pits and react with hydroxyl ions to produce hydroxide. The concentration of chlorides inside the pit triggers a different mechanism of propagation that advances the corrosion inward into the metal, rather than on the outer surface. This results in a decrease in pH due to the increasing number of dissolved acids, which makes the passive film more susceptible, while the pH in cathodic regions (outer surface) increases, forming a film that cannot be penetrated. The overall reaction of pitting corrosion can be written as.

$$M^{y+} + yH_2O \rightarrow M(OH)_y + yH^+$$

It is critical that pitting corrosion creates stress-concentrated zones, making the material weaker to other types of failure. Pitting corrosion can also act as a precursor for crack initiation and propagation, causing fatigue or stress-corrosion cracking mechanisms.

Figure 35: Pitting corrosion at the ship's hopper tanks.

Retrieved from: https://officerofthewatch.com/2013/12/06/corrosion-pitting-on-ships-side/

6.2.3 Crevice

The type of corrosion that occurs at the crevices of metal is known as crevice corrosion and it affects specific areas on the surface. This type of corrosion is particularly hostile for active-passive metals and alloys such as stainless steel, titanium, and aluminum alloys that are widely used. Crevice corrosion is commonly found under deposits, at welds, and between two metal surfaces or between a metal surface and a non-metallic surface. The corrosion is caused by the trapped solution in these regions, leading to wear and failure in mechanical elements or structures. The phenomenon starts due to the presence of dissolved oxygen, particularly due to the driving force from the difference in oxygen concentration between the aggressive solution in the crevice and the outer surface. This difference transforms the crevice into an anode, due to the loss of oxygen, and the outer surface into a cathode. The lack of oxygen attracts chloride ions, which increase and cause corrosion. As the concentration of chlorides increases, the corrosion is intensified through the acidification of these ions during hydrolysis, which lowers the pH of the solution, leading to further destruction of the anode while protecting the cathodic outer surface.

Figure 36: Crevice corrosion thrives at areas around nuts.

Retrieved from: https://www.corrosionpedia.com/whats-the-inside-scoop-on-crevice-corrosion/2/6588

6.2.4 Galvanic

Galvanic corrosion occurs when two dissimilar metals come into contact through an electrolyte, such as seawater. Since these metals are submerged under the surface of the water, the driving force that causes corrosion is the potential difference between them. This electrochemical reaction involves the transfer of electrons between the two electrodes, the anode and cathode. The metal that exhibits corrosion is the anode or the active one, while the other metal is the cathode or the more noble and inert one, according to the galvanic series table. It is noteworthy that combining metals with a significant potential difference, i.e., with a considerable distance in the galvanic series or with a high ratio of surfaces, leads to further corrosion attack. The active metal undergoing corrosion releases electrons that are consumed on the surface of the passive metal. Hence, when these two metals are under an electrolyte, the active material protects the inert one.

Galvanic corrosion plays a significant role in the marine industry as ships and offshore constructions are mostly made of steel. In order to protect the part of the ship that is immersed, active materials are attached to its hull (Zn or Mg), converting the surface of the steel plain into a cathode. This way, by placing a more active metal on the hull, it attracts oxidation and acts as a defense measure against corrosion.

Figure 37: The sacrificial anodes at the hull.

Retrieved from: https://thenavalarch.com/ship-corrosion-cathodic-protection-sacrificial-anodes/

6.2.5 Stress-Corrosion

Stress Corrosion Cracking (SCC) affects materials that are subjected to tensile stress in a corrosive environment. The stresses are a result of both external loadings and residual stresses that result from deformation processes. Like fatigue, the material undergoes stresses that are below its yield strength in the elastic region, making the Linear Elastic Fracture Mechanics (LEFM) applicable. According to this theory, the stress magnitude is dependent on the material's intensity factor K_I, while the crack grows at a rate of $\frac{d\alpha}{dN}$ per cycle. Stress corrosion occurs at specific combinations of materials, environment, and loads. The most common examples are:

- Stainless steel interacting with dissolved chlorides but not in ammonia environment
- Brass and other copper alloys exhibit SCC in presence of ammonia but are not affected by the existence of chlorides
- High strength ferritic steels in damp environment
- Carbon steels are influenced by nitric acids and solutions with pH above 7 (alkaline solutions) however, they remain intact under ammonia or chlorides solutions.

The stress corrosion cracking is primarily explained by two mechanisms: slip dissolution and hydrogen embrittlement. Slip or crack edge dissolution refers to the process where the active crack progresses as a result of the anodic dissolution of its tip, while the material's outer surface remains passively protected. The crack is active because the applied stress creates an acute imperfection that results in the formation of slips, which uncover a renewed metal surface that is no longer passive. Thus, the corrosive environment, particularly the presence of chlorides, contributes to the crack's advancement by destroying the protective layer within the defect.

The hydrogen embrittlement mechanism is based on the buildup of atomic hydrogen at the crack's edge due to the cathodic reaction. The cathodic process, such as the cathodic reaction of water disintegration, which is a major source of hydrogen, generates atomic hydrogen that accumulates at the crack's tip and spreads to the dislocations. This results in subsequent fractures at the edge of the crack, weakening the bond and causing the flaw to expand.

From fractography perspective, the mechanism of SCC resembles brittle fracture in terms of the appearance of the ruptured surfaces. The broken pieces are rough and covered in a thick layer of corrosion products. The outer surface often shows evidence of corrosion, including pits and branches, but it is not as affected as the ruptured surfaces. Additionally, stress corrosion results in crack propagation, which can only be observed through microscopic analysis. The direction of the cracks is determined by the most energetically favorable path, often along the intergranular propagation. However, the cracks can also spread across the grains due to transgranular proliferation. The presence and shift between these two types of fracture depends on the energy of the grain boundaries. When the boundaries have low energy, a protective film cannot form and intergranular fracture occurs. When the grains are actively corroded, the crack follows a direction across the dissolved anodic grains, resulting in transgranular rupture.

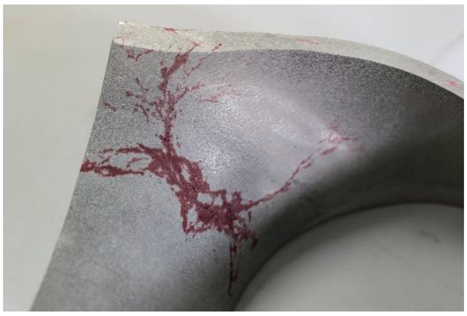

(a)

(b)

Figure 38: (a) SCC at a stainless steel exposed to marine environment, (b) intergranular SCC at microscopic level.

Retrieved from: (a) https://www.warrenforensics.com/2021/01/29/stress-corrosion-cracking-of-stainless-steel-in-marine-environments/ and (b) https://www.ampp.org/technical-research/impact/corrosion-basics/group-3/stress-corrosion-cracking

6.2.6 Cavitation

Cavitation refers to the boiling of a fluid at normal temperature when the static pressure is low enough. It is a form of corrosion that leads to constant wear and tear on machinery equipment such as pumps and turbines, as well as on ship propellers. The dynamic movement of the propeller blades causes a decrease in the local static pressure below atmospheric pressure, leading to the occurrence of cavitation. The presence of dissolved gases released due to the decreased pressure exacerbates the adverse effects of cavitation. As a result, the cavitation voids or bubbles that form during this process converge into high-pressure zones where they then collapse. The condensation occurs rapidly as the surrounding fluid impacts nearby walls or liquids as the voids collapse. This creates a shock wave with a magnitude level of 400Mpa, temporarily increasing pressure in that area before ending. The repetitive breaking up of voids near solid surfaces leads to cavitation, which is associated with a number of failures such as fatigue, material detachment, cavities, and pits [51].

Figure 39: The formation of cavitation during the propeller's movement (left) and the outcome of the cavitation's impact (right).

Retrieved from: https://www.godownsize.com/why-do-boats-cavitate-explained/ and https://www.britannica.com/technology/naval-architecture/Cavitation

7. Fatigue

Fatigue is a mode of failure that occurs when structures are subjected to cyclic loading. In comparison to static loading, the material fractures under significantly lower stresses than its yield strength. The fact that this is not easily observed leads to numerous accidents. Fatigue does not cause sudden failure, but rather it occurs over a prolonged period of recurrent stress or strain that oscillates between a maximum and minimum value. The progressive accumulation of damage is responsible for the initiation and propagation of cracks, and under certain conditions related to its critical length, it leads to final rupture. The concept of fatigue life, N_f which refers to the total number of cycles to failure, is an important consideration in measuring the adverse effects of fatigue. According to this, the progression of fatigue is divided into four stages: the accumulation of plastic deformation, crack initiation, crack propagation, and fast fracture. The first two stages, associated with the cycles required to initiate a crack, form the first phase of the aggregate fatigue life, N_i. The second phase, N_p, refers to the necessary cycles for the proliferation of the crack and the fracture. Therefore, the fatigue life is calculated as $N_f = N_i + N_p$.

There are two approaches to predict failure. The first is related to strain life and assumes that there are no pre-existing cracks in the material. This method classifies fatigue as low-cycle fatigue (LCF) and high-cycle fatigue (HCF). The main difference between these two is the number of cycles required for failure. During LCF, extensive plastic deformation occurs due to high stress, and the life is less than 10^4cycles. On the other hand, HCF is more than 10^4cycles due to low stress, primarily causing elastic strain.

The second approach assumes the presence of pre-existing cracks due to imperfections during material production and processing or jointing during welding. This method, called damage tolerance, requires N_i=0, and the lifecycle depends on the number of cycles required for the critical length of the crack, N_f=N_p. Additionally, damage tolerance is closely related to the theory and basic problem of fracture mechanics [52].

7.1 Cyclic Behavior

Fatigue is a phenomenon caused by the repeated application of stresses that vibrate between a maximum and minimum value. This cyclic loading is described by parameters such as the maximum stress range, $\Delta\sigma = \sigma_{max} - \sigma_{min}$, the mean stress $\sigma_m = \frac{\sigma_{max}+\sigma_{min}}{2}$, the stress amplitude $\sigma_\alpha = \frac{\Delta\sigma}{2} = \frac{\sigma_{max}-\sigma_{min}}{2}$, and the stress ratio R=$\frac{\sigma_{min}}{\sigma_{max}}$ (R= -1 for completely reversed loading, R=0 for zero-tension fatigue, and R=1 for static loads). When a specimen is subjected to low-cycle and high-cycle fatigue, the plastic deformation that occurs under high stresses affects the relationship between stress and strain, transforming them into a non-linear form, which is described by a hysteresis loop.

In the case of monotonic tension, a cylindrical specimen fractures under gradually increasing static loads. The stress and strain for the elastic region are defined as $\sigma = \frac{F}{A_0}$, $\varepsilon = \frac{l-l_0}{l_0}$, and are associated with Hooke's law, $\sigma = E\varepsilon$. The total strain is the sum of plastic and elastic strain $\varepsilon = \varepsilon_p + \varepsilon_{e.}$. After reaching the yield point (σ_y), plasticity begins and the curve until the point of necking (σ_{uts}) is described by Hollomon's equation, $\sigma = K\varepsilon_p^n$,, where K is the stress hardening coefficient and n is a strain hardening exponent. In the plastic region, the true values of stress and strain are expressed as $\sigma = \frac{F}{A_i}$ and $\varepsilon = \int_{l_0}^{l} \frac{dl}{l} = \ln(\frac{l}{l_0})$. Thus, according to Ramberg-Osgood, the monotonic stress-strain diagram is shown by the expression $\varepsilon = \frac{\sigma}{E} + (\frac{\sigma}{K})^{\frac{1}{n}}$.

Bauschinger showed that during a cyclic stress-strain test, the strength of a material until plastic deformation occurs under tension is diminished when compression loads are applied and vice versa. Fatigue is usually detected in regions where geometrical discontinuities exist, leading to permanent strain after a certain stress level. The area inside the hysteresis loop indicates the amount of energy lost per cycle. As shown in Fig.40 the area inside the hysteresis loop indicates the amount of heating energy (plastic work) that has been lost per cycle. Before the loop stabilizes after a certain number of cycles, there is a temporary stage in which fully annealed materials exhibit cyclic hardening behavior, while cold-worked materials show cyclic softening behavior. Cyclic hardening is related to higher stress level that is necessary for bring forth the same strain per cycle while cyclic softening is associated with the opposite process, when it is required a lower stress level in order to churn out the identical strain as well.

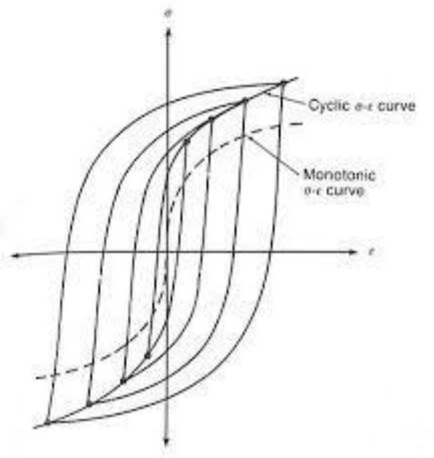

Figure 40: The hysteresis loop.

Retrieved from: http://glastonburyli.weebly.com/uploads/1/2/7/3/1273419/12_fatigue_of_metals.pdf

The stabilized hysteresis loop is expressed based on the true elastic strain amplitude $\Delta\varepsilon_e$, the true stress range $\Delta\sigma$, and the true plastic amplitude $\Delta\varepsilon_p$. The combined strain range is written as $\Delta\varepsilon = \Delta\varepsilon_e + \Delta\varepsilon_p = \frac{\Delta\sigma}{E} + \Delta\varepsilon_p$. Combining the above assumptions and conducting experiments through, principally, three methods (companion, incremental step and multiple step method) it leads to a large number of stabilized loops that form the cyclic stress-strain curve. Hence, likewise the monotonic tension but in this occasion based in true stress and strain amplitudes the cyclic curve can be expressed as, $\varepsilon_a = \frac{\sigma_\alpha}{E} + (\frac{\sigma_\alpha}{K'})^{\frac{1}{n'}}$, where $\sigma_\alpha = K'(\frac{\Delta\varepsilon_p}{2})^{n'}$ is the relation between the strain and stress range. Hard materials will lose strength due to the repositioning of dislocations, while soft materials will be hardened due to an increase in dislocation numbers [53].

7.2 Stress Life (S-N Curve)

This method was developed by Wohler in 1860 through experiments aimed at determining the material properties under fatigue. After several bending load tests, the results were plotted on a S-N diagram that shows the relationship between applied stress and the number of cycles to failure. As shown in the diagram Fig. 41, the approach is typically used in the elastic region where fatigue life exceeds 10^3cycles and it is noted that higher stress levels result in fewer cycles to fracture. The fatigue limit or endurance limit is the highest stress level under which the material will not fail and represents the greatest stress the material can withstand over an infinite number of cycles.

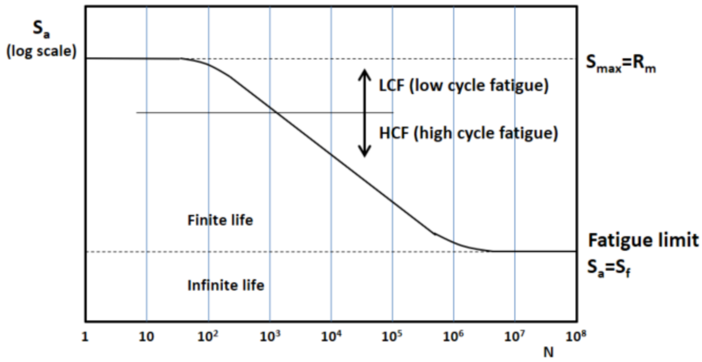

Figure 41: The S-N diagram.

Retrieved from: https://www.fatec-engineering.com/2018/02/20/description-of-a-s-n-curve/

Many materials, especially non-ferrous ones, are described by fatigue strength, which refers to the stress level required for failure after $N_f = 10^7$cycles. When the results of the S-N diagram are plotted on a log-log scale, a linear correlation is observed between fatigue life (N_f) and true stress amplitude. This formula, developed by Basquin in 1910 through a fully-reversed and consistent stress range fatigue analysis, is given as

$$\frac{\Delta\sigma}{2} = \sigma_\alpha = \sigma_{f'}(2N_f)^b$$

Where $\sigma_{f'}$ is the fatigue strength coefficient and b is the Basquin exponent, which fluctuates between -0.12<b<-0.05 for most metals. It should be noted that the above relation requires fully reversed loading and zero mean stress (R=-1), which cannot be implemented in all cases. Furthermore, mean stress σ_m has a significant impact on the fatigue life, most commonly in the elastic region, and influences material behavior.

Morrow (1968) suggested a modified form of Basquin's relation for nonzero mean stress, which is $\sigma_\alpha = (\sigma_{f'} - \sigma_m)(2N_f)^b$and the life of a material is given by the expression $N_f = (1 - \frac{\sigma_m}{\sigma_{f'}})N_f|_{\sigma_m=0}$. An increased mean stress, either tensile or constant, leads to a decrease in strength coefficient and fewer cycles. On the other hand, applying compressive stress enhances the fatigue life.

When $\sigma_m \neq 0$, it is crucial to determine a substitute stress amplitude that will result in the same number of cycles as the true stress amplitude. The most noted theories were established by Gerber in 1874, Goodman in 1899, and Soderberg in 1930.

- Goodman's expression $\sigma_\alpha = \sigma_\alpha|_{\sigma_m=0}\{1 - \frac{\sigma_m}{\sigma_{uts}}\}$, where σ_{uts} is the ultimate tensile strength
- Soderberg's relation $\sigma_\alpha = \sigma_\alpha|_{\sigma_m=0}\{1 - \frac{\sigma_m}{\sigma_y}\}$, where σ_y is the yield strength
- Gerber's equation $\sigma_\alpha = \sigma_\alpha|_{\sigma_m=0}\{1 - (\frac{\sigma_m}{\sigma_{uts}})^2\}$,

The expressions mentioned above are illustrated in Fig. 42. The Soderberg equation relates to a conservative estimate of fatigue life, while Goodman's expression is ideal for brittle materials and conservative for ductile ones. It is notable that under compressive mean stress, the equation is non-conservative, so to overcome this issue, this stress is considered negligible for fatigue life. Gerber's equation effectively describes fatigue life under tensile mean stress, but disregards the adjustments caused by changes from tensile to compressive mean stress. The S-N curves depend on the type of loading (axial, bending, torsion), stress concentration, and notch sensitivity. Factors such as K_t, K_f *and* q have been developed to encompass these features. In the case of combined effects, the stress amplitude and mean stress can be written as a combination of these coefficients.

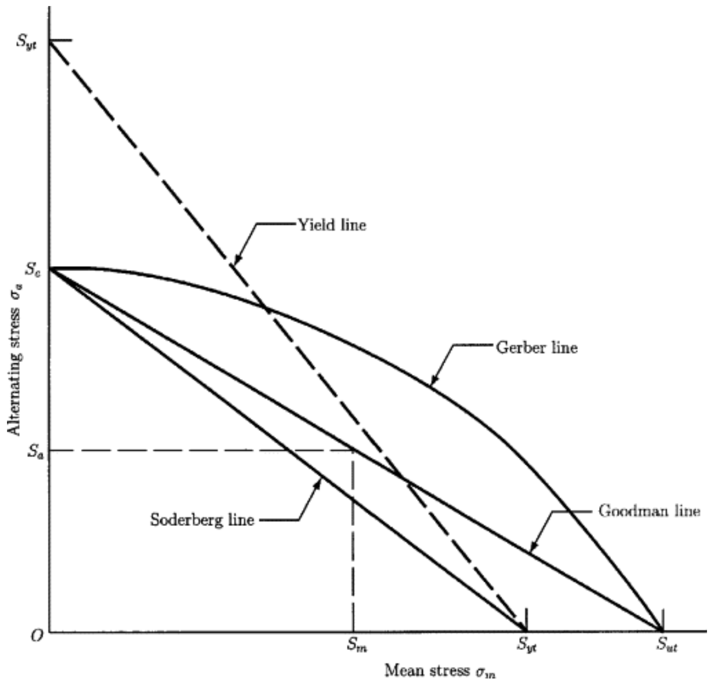

Figure 42: The comparison of the different expressions.

Retrieved from: https://www.sciencedirect.com/topics/engineering/goodman-diagram

The above analysis implies a constant stress amplitude during cycle loading, but most materials or elements are inevitably subjected to a range of stress amplitudes and mean stresses. Considering different parts of loading, each section has its unique stress amplitude $\sigma_{\alpha i}$ and number of cycles n_i. According to Miner (1945), who developed the theory for cumulative damage, the criterion for predicting failure under these circumstances should take into consideration the total amount of linear damage and compare it with a key magnitude. The main drawback is that the theory omits the sequence of each part of the cyclic loading, so the failure could occur below the critical value if the amplitude of a specific part causes more damage than expected. Hence, Miner's rule necessitates considering the sequence of cyclic loading,

$\sum_{i=1}^{m} \frac{n_i}{N_{fi}}$, where N_{fi} is the number of cycles required for failure [54].

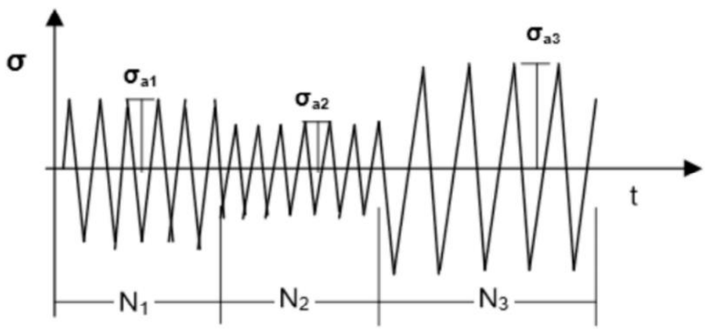

Figure 43: Time history of the stress amplitude change.

Retrieved from: https://www.researchgate.net/figure/Scheme-of-use-hypothesis-Palmgren-Miner-to-sum-of-fatigue-damage-a-mark-for-the-time_fig4_331939351

7.3 Strain Life (HCF and LCF)

The previously presented approach is widely used when permanent deformation is considered to be insignificant. In the case of high loads, the material undergoes a lower number of cycles before failure, as a result of plasticity. The Strain Life approach describes this behavior, including phenomena that occur in the plastic region, while introducing the strain-life curve, which replaces the S-N diagram. The method assumes that the material has no pre-existing cracks, so the fatigue life is given $N_f = N_i + N_p$ The percentage of fatigue life consumed to initiate a crack, N_i ranges between 0% for materials with extremely high stress concentrations due to rough surfaces and imperfections, and 80% for seemingly ideal, flawless materials.

High-Cycle Fatigue (HFC) is associated with a large number of reversals before failure, approximately $N_f > 10^4$, as it occurs in the elastic region. For example, the waves and wind that a ship or other marine structure is subjected to, form long-term loadings, which are relevant to HFC. The elastic zone is well described by Basquin's rule, as stated in the stress life method. Materials that can withstand modest amounts of strain and provide an extended life under these conditions are usually high strength. This mode of fatigue is described by the aforementioned S-N diagrams, which infer the factors that have a significant impact on fatigue life.

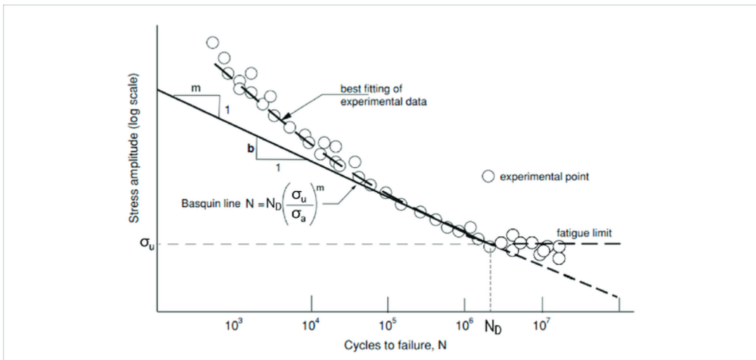

Figure 44: The Basquin's equation diagram.

Retrieved from: https://www.researchgate.net/figure/S-N-Curve-regarding-to-the-Basquin-theory-with-the-slope-m-from-Milella-2012-s-u_fig1_364237622

Fatigue related to significant plastic strain is known as Low Cycle Fatigue (LCF) and is correlated with a low number of cycles before failure, $N_f < 10^4$. In the marine industry, LCF can be found in offshore structures as a result of exposure to a block of waves during storms, or in ships during an operation of unloading and loading cargo [55]. Coffin-Manson (1953) established an expression to define the relationship between plastic strain and fatigue life, which can be linear on a log-log scale diagram. This equation is written as, $\frac{\Delta\varepsilon_p}{2} = \varepsilon'_f(2N_f)^c$, where $\frac{\Delta\varepsilon_p}{2}$ is the plastic strain amplitude, ε'_f is the fatigue ductility factor, and c is an exponent related to fatigue ductility, varying between -0.7 and -0.5 values. By combining the Coffin-Manson law with Basquin's equation and considering that the total strain can be analyzed into elastic and plastic components, the expression that describes the material behavior under LCF and HFC is, $\frac{\Delta\varepsilon}{2} = \frac{\sigma_{f'}}{E}(2N_f)^b + \varepsilon'_f(2N_f)^c$ (*). As shown in Fig. 45, the curve that characterizes the total behavior is asymptotically converging to the separate curves. The region between 10^4 and 10^5cycles, where the LCF curve intersects the HFC curve, implies that the elastic strain amplitude is equal to plastic in equation (*) and the transition reversals are given by $2N_t = (\frac{E\varepsilon'_f}{\sigma_{f'}})^{\frac{1}{b-c}}$. When the number of cycles is lower than the transition level, there is a presence of large strains following plastic deformation, so an enhanced fatigue life depends on the property of ductility. Tough metals have ideal strain-life performance, as they are a combination of adequate strength and ductility [56].

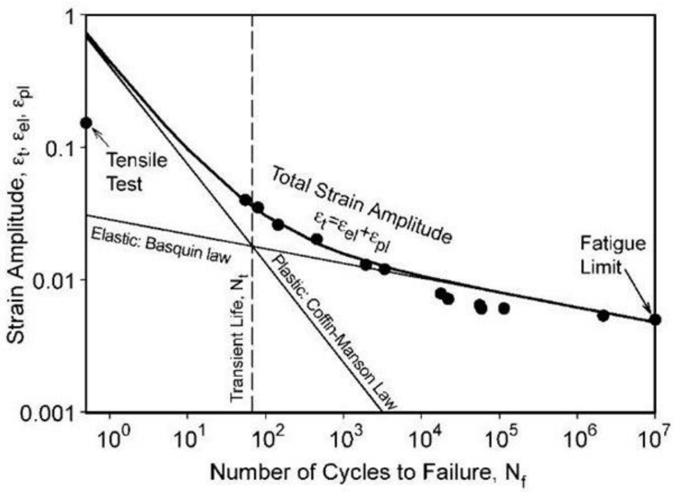

Figure 45: Strain-Life diagram.

Retrieved from: http://what-when-how.com/nanoscience-and-nanotechnology/nanocrystalline-materials-fatigue-part-1-nanotechnology/

7.4 Damage Tolerance

Marine structures endure fatigue that results in crack propagation, mainly at welded parts, due to repeated cyclic loading. These areas often contain imperfections and pre-existing cracks due to manufacturing defects, which can compromise the structure's integrity and cause negative consequences. To address this, Damage Tolerance Analysis is widely used to detect the presence of flaws and evaluate the structure's remaining strength and fatigue life. The total number of cycles required for a crack to reach its critical value is denoted as $N_f = N_p$. Non-destructive testing (NDT) techniques, such as visual inspection, leak testing, Magnetic Particle, Eddy Current, Radiography, and Ultrasonic testing, are employed to determine the initial length of cracks a_0 in the most vulnerable welded parts. Of these techniques, Ultrasonic testing is the most reliable and widely used, as it is effective in identifying internal flaws (approximately 70%). If a method is unable to detect the magnitude of a crack, it is considered to have a maximum length that the method cannot distinguish [52].

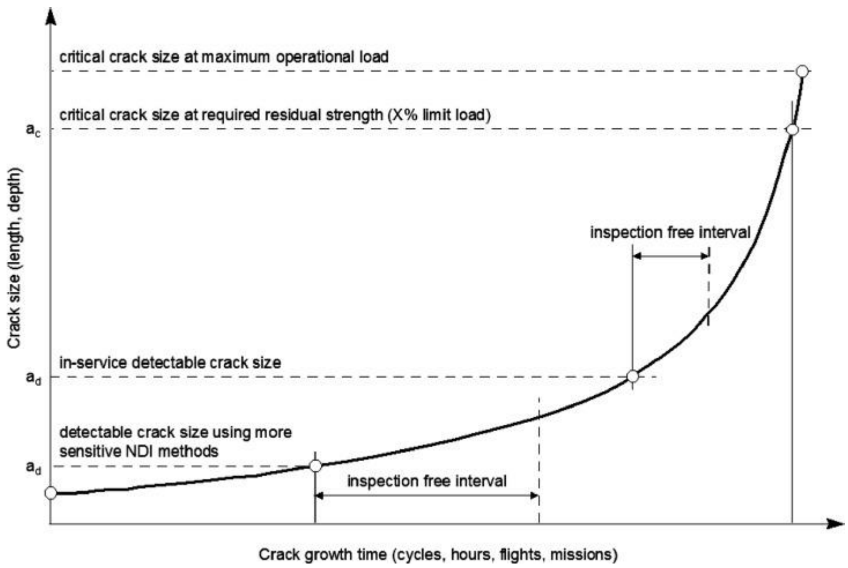

Figure 46: The propagation of the crack.

Retrieved from: https://www.sciencedirect.com/topics/materials-science/fatigue-crack-growth

As shown in the Fig. 46, the crack has an initial length a_0 and grows at a rate of $\frac{d\alpha}{dN}$ until it reaches its critical value, a_f. Damage Tolerance Analysis is based on assumptions made for linear elastic fracture mechanics (LEFM). In this framework, for a notched structure with a pre-existing crack length α subjected to cyclic loading, the maximum and minimum stress intensity factors (K_{max}, K_{min})are related to the maximum and minimum stresses ($\sigma_{max}, \sigma_{min}$), respectively. The stress intensity factors can then be written as follows:

$K_{max} = F\sigma_{max}\sqrt{\pi\alpha}$

$K_{min} = F\sigma_{min}\sqrt{\pi\alpha}$, where F is a coefficient related to geometry and stress conditions.

The stress intensity factor range is specified as ΔK= K_{max} - K_{min} = ($\sigma_{max} - \sigma_{min}$) =Δσ$\sqrt{\pi\alpha}$. Plotting the experimental results in a log-log scale the correlation between the growth rate $\frac{d\alpha}{dN}$ and the ΔK is depicted in Fig. 47. The sigmoidal diagram is divided into three regions. The first region describes crack initiation, where for small values of ΔK, the crack will not expand if it is below the threshold $(\Delta K)_{th}$. The second region entails crack propagation in a linear form, which was developed by Paris-Erdogan in 1963. This law indicates that the crack growth rate is a linear function of the stress intensity factor range and is expressed as,

$\frac{d\alpha}{dN} = C(\Delta K)^m$ where C and m are material constants. The third region represents the unstable condition of the crack under an excessive value of ΔK and the final rupture.

The crack propagation and its critical length rely on the material critical stress intensity factor K_{IC} (mode I) which is formed as $K_{max} = F\sigma_{max}\sqrt{\pi a_f} = K_{IC}$. According to Paris-Erdogan expression the life estimation from the initial crack until its critical value is given by $N_f = \frac{[1-\left(\frac{a_0}{a_f}\right)^{\frac{m}{2}-1}]}{C\left(F\Delta\sigma\sqrt{\pi}\right)^m(\frac{m}{2}-1)a_0^{\frac{m}{2}-1}}$. This relationship demonstrates that, in the case of an increased stress range $\Delta\sigma$, the N_f would be reduced. However, if the initial crack is decreased due to improved welding quality, appropriate treatment, or improved NDT means, the N_f will expand, as it does when the critical length a_f increases following the growing value of K_{IC} [57].

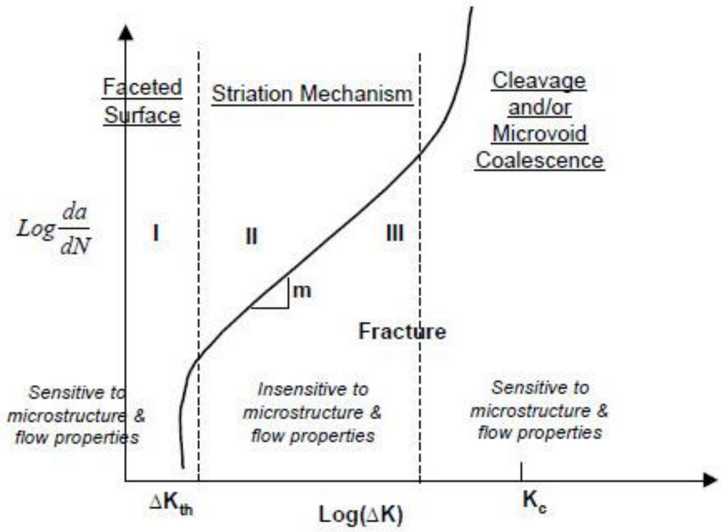

Figure 47: The three stages of fatigue.

. Retrieved from: https://www.totalmateria.com/page.aspx?ID=CheckArticle&site=kts&NM=299

7.5 Fractography

Fatigue is a failure mechanism that can cause fracture under repeated cyclic loading, even when the load is below the yield strength in the elastic region. This process is influenced by environmental conditions, stress concentration, microstructure, load history, and surface quality. The crack propagation changes during each stage, providing valuable insight into the origin and progression of fracture and the impact of external factors such as the environment and loading form. At the macroscopic level, there are signs that reveal the influence of stresses and operating conditions, known as beach or clam shell marks. Striations, which are curved lines appearing during the second stage, seem to originate from a center that indicates the location of crack initiation. The final rupture, which is the third stage, results in a rough and lean surface.

The first stage involves the initiation and gradual progression of a crack. The origin of the crack is commonly found in areas of stress concentration, such as at sharp edges, notches, and gaps. This stage does not show significant macroscopic characteristics because it is influenced by the material's microstructure and grain size. The crack size and plastic zone are proportional to the grain size, thus limiting the crack's spread. Beach marks serve as limits during the first stage, restricting the crack's slow growth. To analyze crack formation at the microstructural level, Wood's method, also known as intrusion and extrusion, is widely used. According to this method, the leading slip plane experiences intermittent slipping that creates extrusions on surfaces where dislocations move smoothly. To maintain the material's continuity, the opposite process takes place, causing dislocations to push material inward, creating an intrusion. When an intrusion reaches a certain size and shape, it transforms into a crack. Forsyth developed a variation of Wood's method, stating that in perfect surfaces of ductile materials, extrusions are densely packed, allowing a nearby slip strip to cause decohesion and form cracks.

Figure 48: Example of fatigue fracture surface.

Retrieved from: https://www.phase-trans.msm.cam.ac.uk/2017/ff.html

The second stage refers to the propagation of cracks in relation to the fatigue crack growth rate $\frac{d\alpha}{dN}$ and generally results in a smooth appearance. When the plastic zone reaches a size that consists of many grains, it implies that the crack spreads steadily in a plane that forms a 45º angle with the applied stresses, leading to transgranular, non-crystalline rupture. The macroscopic level is illustrated by beach marks, which describe the propagation that occurred either due to the modification of stress amplitude or environmental changes. As demonstrated in Fig. 49, beach marks are situated at the outer edges of the fracture frame due to the presence of a high growth rate in the middle area of the thickness located in plain strain. At the microscopic scale, the presence of striations suggests that the failure mechanism is fatigue, but not vice versa. It is believed that each striation represents a load cycle, and its shape depends on the material properties. Ductile materials have sleek, wave-like striations, while brittle materials have an uneven, toothed shape. The final, unstable stage is affected by the rapidly growing stress state, causing rupture. As the maximum intensity factor approaches the critical value, the microstructure affects the material in the same way as it does with its toughness [58].

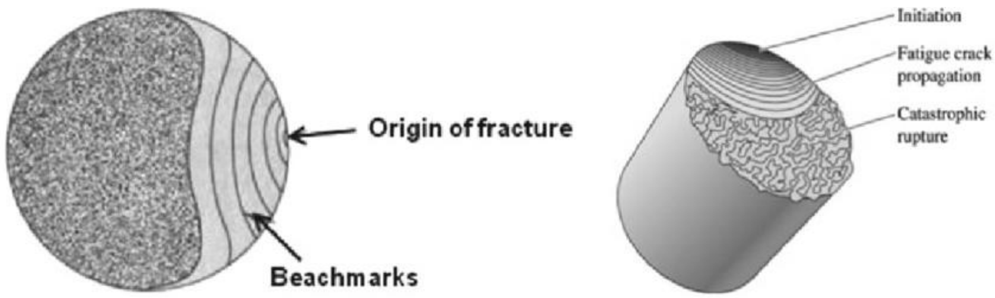

Figure 49: Fatigue fracture with benchmark (left) and fatigue crack initiation and propagation (right).

Retrieved from: https://www.researchgate.net/figure/Schematic-representation-of-fatigue-fracture-surface_fig2_325467396

8. Case Studies

8.1 Liberty Ships

During World War II, the USA implemented an extensive shipbuilding program to meet the supply demands of the war. During this period, 18 new shipyards were built to support this ambitious plan, which included the mass production of ships capable of carrying all essential equipment needed in wartime. Between December 1941 and October 1945, 2,711 all-welded Liberty ships were constructed. The Emergency Fleet Program was based on two fundamental principles: simplicity and adaptability. The shipbuilding plan utilized extensive prefabrication and welding, as well as the implementation of production-line techniques. Many components of the ships were built on the mainland, as the new shipyards lacked essential tools and equipment. These ship parts were transported by trains or other means to the yards for welding. At that time, Americans had little knowledge about welding processes, while dominant shipbuilders such as Europeans and Japanese used the riveting method to join the parts of a ship. However, Americans found that welding, in combination with the production line, could save significant time in building ships.

Figure 50: Liberty ships, the cornerstone of USA Merchant Marine Transport during WWII.

Retrieved from: https://www.warhistoryonline.com/instant-articles/liberty-ships.html?chrome=1

The design of the Liberty ships relied on previous designs for a series of ships known as the Ocean Class. This design was modified by the U.S. Maritime Commission and its chairman, Emory Scott Land, who was responsible for naval architecture and construction during World War II. The first keel of the Liberty ships was laid on April 30, 1941, in Maryland, and five months later, on September 27, the first vessel named "Patrick Henry" was launched, inaugurating the wide shipbuilding program. That day went down in history as Liberty Fleet Day, as the master of the program, Emory Scott, said. The Liberty ships had a nickname that U.S. President Franklin Delano Roosevelt attributed to them and spread throughout the country: "The Ugly Ducklings." In November 1942, a record was set when the Liberty ship called "Robert E. Peary" was launched after four days and 15 hours of construction.

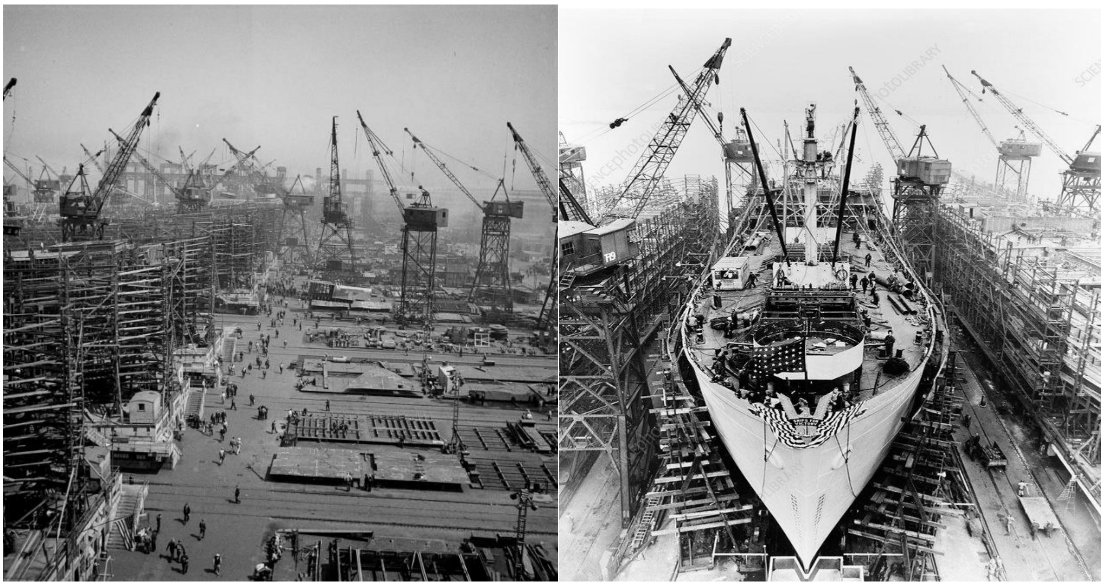

Figure 51: Liberty ships under construction.

Retrieved from: https://rarehistoricalphotos.com/building-liberty-ships-1941/

The dimensions of the Liberty ships were: 134.6m in length, 17.4m in breadth, 11.38m in depth, and 8.46m in draught. They had 7176 gross register tons, 4380 net register tons, and 10865 tons deadweight. Furthermore, the ship had five cargo holds: three forward from the accommodation located midship, and two aft holds behind the accommodation. The overall capacity of the cargo holds was approximately 562,608 cubic feet of wheat. To load the cargo, the ship was equipped with three masts that supported booms for cargo handling. The machinery equipment was located below the accommodation and consisted of two boilers and a triple expansion steam engine. The ship had a single propeller that provided a velocity of around 11 knots.

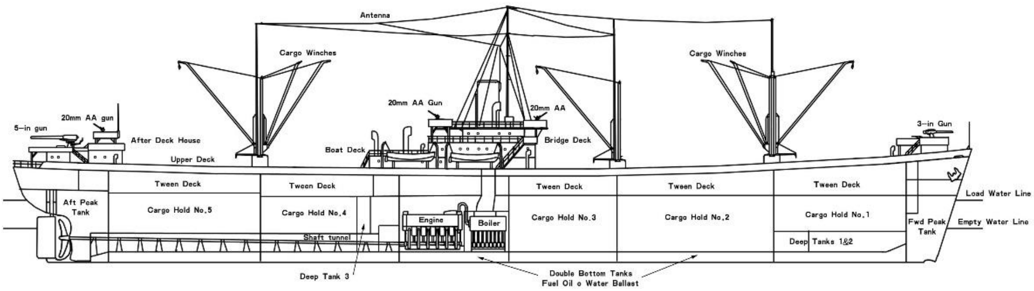

Figure 52: The ship design.

Retrieved from: https://www.navalgazing.net/Liberty-Ships-Part-2

During the war, the demand for oil transport increased, thus creating an immediate need for building tanker ships in order to carry liquid cargo. However, there were no available yards for this project, as all of them were occupied by the emergency fleet program. Hence, the U.S. Maritime Commission approved the modification of 62 Liberty ships into tanker ships. This was achieved by installing 9 tanks into the cargo holds, while five ballast tanks in the double-bottom were used for oil transportation. The design of Liberty ships allowed for modification according to the specific needs that emerged during hostilities. Liberty ships could also be utilized as troopships, floating hospitals, transporting aircrafts and carrying the army's animal and other equipment.

After the end of the war, Liberty ships were distributed to allies to strengthen their merchant fleets. Greece also received about 106 Liberty ships as an exchange for its contribution to the war and its destroyed merchant navy. By the end of the 1960s, Liberty ships were sent to scrapyards as modern ships established a new era for the shipping industry. Nonetheless, the Liberty ships inspired the Japanese, who are pioneers in the shipbuilding industry, as they adopted some important techniques used during Liberty production to facilitate fast and easy mass production [59].

8.1.1 The Failure

The mass production of Liberty ships and their widespread use resulted in devastating accidents that led to partial failure and complete breaking of the ships' structure. A total of 1,031 incidents, including cracks, and 200 ships that broke in half or could not be repaired without warning or prior indications, demonstrate the imperative need to understand the root causes of the failures, such as poor welding, properties of the steel used, short construction time, and lack of quality control.

The Liberty ships endeavor highlighted the importance of brittle fracture in constructions, as well as the significance of creating a method that could enable the safe design of structures to prevent brittle fracture, which is one of the most hazardous types of ruptures due to its sudden and disastrous consequences. Hence, a new field, Fracture Mechanics, was developed to provide useful information for preventing rupture. In this direction, the mass production of Liberty ships was an enormous experiment that revealed important issues related to structures and brittle failure, as well as the lack of knowledge or awareness about several connected issues.

In January 1943, the T2 tanker named "Schenectady" was docked at the shipyard where it was built in Oregon, USA. The ship had successfully completed her sea trials and was ready for her first mission. The 152m vessel was moored at a harbor where the water temperature was 4°C, the water was still, and the air temperature was -3°C. Suddenly, the ship broke into two separate parts amidships without any prior warning, accompanied by a loud sound. A similar accident occurred at New York when the liberty ship "Manhattan" approached the harbor and suddenly failed in two pieces during sailing. A total of seven ships experienced a similar failure.

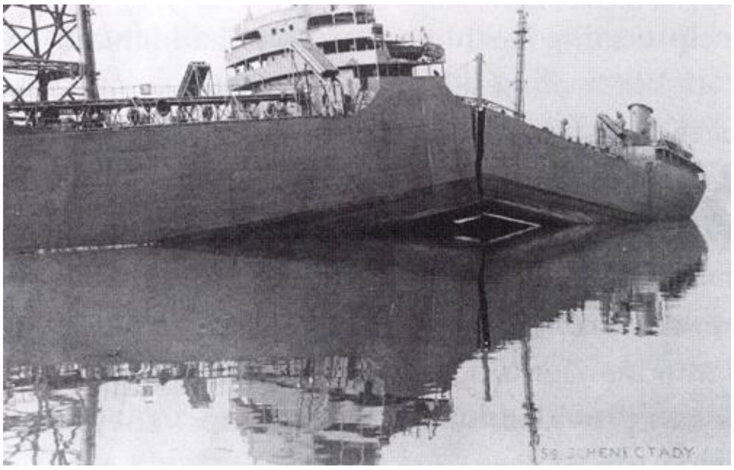

Figure 53: The SS Schenectady T2 tanker.

Retrieved from: https://www.twi-global.com/media-and-events/insights/schenectady-t2-tanker

After several investigations, a report was issued which concluded all the root causes of the failure of liberty ships. The report suggested modifying the ship's design to reduce stress concentrations in parts of the ship that were noticed to be problematic, as well as improving the welding quality to diminish initial flaws and residual stresses. However, the report did not take into consideration the steel properties and fracture toughness of the material, which could lead to brittle fracture. Therefore, it was claimed that the root causes were the low weldability of the steel used for ship construction, as well as stress concentration due to deficient design and poor welding (initial defects) [60].

The main problem that had to be understood was how tough steel could fail easily, while the laboratory experiments indicated high plastic flow and toughness. This was proven by the scientist Dr. Constance Tipper, who was working at Cambridge University. She showed that the conditions in the laboratory are not representative of the conditions in which ships operate. Tipper conducted many experiments to indicate that the energy required for crack propagation at low temperatures in the Atlantic Ocean allows cracks to proliferate more easily than at room temperature. Dr. Tipper used the Charpy test to associate the absorbed energy with temperature, and she laid the foundations for giving a lot of attention to the importance of absorbed energy rather than estimating stresses.

The tests showed that the steel utilized for liberty ship construction experienced the Ductile to Brittle Transition Temperature (DBTT). Brittle fracture thrives at low temperatures under high stress and multi-axial stress constraints. As the temperature decreases, the steel undergoes a change in behavior from ductile to brittle. It is important to define the transition temperature, which is the temperature that corresponds to 20J of absorbed energy according to the Charpy test. As this temperature decreases, the toughness of the steel increases. Thus, a diminished transition temperature is significant in order to avoid brittle fracture.

Nonetheless, the low temperature leads to a reduction in fracture toughness, and the low weldability of the steel exacerbates this reduction. Hence, brittle failures in Liberty ships were due to welded parts that had low toughness and low temperature characteristics, and the cracks initiated from weld flaws or stress concentration regions.

In some instances, residual stresses resulting from welding were the root cause of the failure [61].

It was found that the transition temperature of Liberty Ships' steel was between 15-65ºC, with a mean temperature of 40°C. It is obvious that this type of steel could irrefutably undergo brittle fracture during winter and spring in the Atlantic Ocean. The T2 tanker Schenectady failed in still waters at 4°C, an extremely low temperature compared to the transition temperature of the ship's plates [62]. The outcomes of the Charpy tests conducted by Constance Tipper showed that there was a wide difference in the steel properties along the ship. Some were tested at 0°C and gave 100J impact energy, while others at the same temperature gave 2J impact energy. This means that some parts of the ship could resist brittle fracture at low temperatures while others could not. Besides that, this ascertains that welding could not be the main cause of Liberty ship failures and incriminates the insufficient steel properties [61].

The Liberty accidents mobilized the scientific community to address the insufficient steel properties and find solutions to enhance the weldability of the steels, i.e., to increase the fracture toughness at low temperatures. Metallurgical aspects contributed to this, such as the low carbon content and the addition of elements like Mn and Si, which curb the action of carbon, sulfides, and phosphorus. These chemical elements increase the transition temperature, thereby reducing fracture toughness. Tipper's contribution was significant, as she highlighted the importance of the microstructure along with the chemical composition in brittle fracture. She was able to prove that even with an acceptable ratio of Mn:C, a poor microstructure consisting of rough grains and stress concentrators could overcome the advantages of the adequate Mn:C ratio, leading to decreased toughness [63].

8.1.2 Conclusion

The failures of Liberty ships brought prominence to brittle fracture and its perilous effects. Although poor welding, including hydrogen embrittlement due to electrode welding in damp conditions, and inexperienced personnel who executed these processes were considered the root cause at first, eventually the material properties had the lion's share of the reasons for these failures.

Steel behavior under low temperature can result in brittle fracture due to changes in its behavior and reduction in toughness. This can be deteriorated by steels with high carbon content, sulfur, and phosphorous, especially older steels with high impurity levels. Additionally, the presence of residual stresses plays a crucial role, as non-stress relieved steel has lower toughness compared to steel that has undergone stress-relieved processes. In addition, thick steel and welded materials with coarse grains are prone to brittle fracture, as they tend to decrease the toughness of the material [64].

A small number of Liberty ships and the ships that were constructed before the war had the same steel that was used for the emergency program. The answer to the question of why these ships had not undergone such extensive failure was undoubtedly the method by which the different parts were joined. In comparison with welding, which is a process that saves significant time during construction, the segments of the ships were linked by rivets. Even if the steel exhibited cracks, the rivets acted as crack arrestors, hence they could not propagate easily and cause total failure. This is because when the crack approached the join between two plates, it would stop as one plate is above the other. In welding methods, the crack could not stop because the plates are joined via metallic bonding and the crack will propagate through the weld.

It is obvious that many methods that are accessible now were not available during the war. Advanced welding quality and the development of non-destructive testing (NDT) to check for possible cracks in welds ensured a big step in quality control that evidently did not exist during the war. The Liberty Ships program went down in history for its innovations in the production line, such as prefabrication and mass production, the introduction of welding methods in ship construction, its painful contribution to the future field of Fracture Mechanic, a field that provides a quantitative assessment of toughness for failure, and a better understanding of the influence of temperature on material toughness [65]. Today, ships are built taking into consideration fracture before yielding, but this knowledge only became feasible in the 1960s. New steel grades were developed to sustain high toughness at low temperatures. Based on existing evidence, the lowest impact-tested grade of steel measures 27J at 0°C, while the highest measures 41J at -60°C [62].

8.2 World Concord

The World Concord ship was built in 1952 by the Vickers Armstrong Ltd shipyard and was the largest crude oil tanker in the world at that time. The ship was 199 meters long, had a load-carrying capacity of 20,125 tonnes gross, which was distributed across the 10 cargo tanks, and was a single-deck, all-welded construction. During its construction, there were a number of advancements in the maritime industry, such as the elimination of the v-notch effect and increased steel toughness requirements, which minimized ship-related accidents. The ship was built according to the ship-making standards of the era and met all safety regulations.

On November 20, 1954, the ship set off bound for Syria, in a winter ballast departure condition, carrying approximately 18,000 tonnes of water ballast, according to the manufacturer's recommendations. Later in the evening, a weather forecast warned of imminent strong gales in the area, so the Master took on even more ballast while simultaneously reducing the engine speed. Disaster struck in the early morning of the next day when wind forces became very strong, and waves up to 10 meters started rising. The ship was struck consecutively by two large waves; the crest of the first wave found the ship directly beneath it, while the other broke over the foredeck. This caused a rumbling sound, and shortly after, the ship broke in half. Fortunately, it remained afloat, and the crew was rescued safely.

Figure 54: The World Concord split in half.

Retrieved from: https://www.twi-global.com/media-and-events/insights/world-concord-tanker

8.2.1 The Failure

The construction of the ship's bottom compartment created two regions of stress concentration related to the longitudinal T-shaped beams. It is believed that the fracture initiated from one of those areas. The fracture was sudden and propagated in a brittle fashion, running along the bottom of the ship through the transverse bulkhead that was amidships, and all around the hull and deck area, which caused the vessel to split in two. The bilge strakes, deck stringers, and sheer strakes were made of steel that complied with the specifications of the 1950s. The rest of the plates were of ordinary shipbuilding quality according to 1950s standards.

The investigation that was conducted to identify the causes of the failure indicated that the V-notch properties of the hull's steel plates were inadequate, with a Charpy energy of only 27J at -12°C, which was the water temperature during the accident. Furthermore, due to the water ballast condition, which was within safety margins, the hull was overstressed, especially the bottom shell plating. Although the ship was an all-welded construction and had a strong potential for initiating failure from a defective weld, it was considered that the combination of low-quality, low-toughness steel used and high-stress levels led to this incident.

8.2.2 Conclusion

The failure of the World Concord led to modifications in the requirements and standards of classification societies regarding the V-notch toughness of steel used in the shipbuilding industry, as well as the need to ensure sufficient welding quality. Lloyd's Register implemented mandatory specifications for the steel, including a Charpy test with 47J absorbed energy at 0°C, and a maximum percentage of chemical elements such as carbon, manganese, phosphorus, and sulfur that can affect the transition temperature and weldability of the steel [4], [66].

8.3 M/T Erika

On the 11th of December 1999, the M/T Erika, a 24-year-old, Malta-registered ship, was travelling from Dunkirk to Livorno, carrying 30,884 tons of heavy oil, when it experienced structural failure during a heavy storm. The ship was travelling at 6.5 knots through harsh weather conditions, with wind speeds of about 7-8 Beaufort and waves reaching heights of 5-6 meters. Immediately after the initial failure, the ship obtained a significant list, and when it returned to a stable state, it broke off amidships after several hours. The crew managed to abandon the ship safely, without reporting any injuries or human loss. The disaster of the Erika ship was in the Bay of Biscay, causing significant ecological catastrophe along the coasts of France due to the hazardous cargo itself and the severe conditions, which impeded the oil spill confinement efforts by the responsible authorities.

Figure 55: The sinking of M/T Erika.

Retrieved from: https://safety4sea.com/cm-learn-from-the-past-erika-oil-spill-europes-environmental-disaster/

The ship had been built in Japan in 1974 and consisted of 13 cargo tanks. It had an overall length of 184.03m, a breadth of 28.05m, and a depth of 14.99m. The commission charged with identifying the root causes of the accident found that the Erika was an obsolete vessel that had not been maintained and inspected for a long period, and was equipped with only the minimum essential equipment.

Prior to the investigation of the accident, the commission ascertained from the ship's reports that the vessel had been inspected at least once per year by the Port State Control authorities. The ship was prohibited from departing twice due to extensive corrosion that had been detected during inspections. Corrosion was also found at least twice in the hull and accommodation departments, without any more specific information about the status of these sections. The last inspection that had taken place before the Erika accident was extremely limited, including only the minimum examination of the vessel's certifications.

8.3.1 The Failure

A sequence of factors has led to the sinking of the ship, resulting in a major environmental disaster and causing detrimental consequences for the marine life in the area. After several investigations, it was found that the ship had been maintained one year before the accident through dry dock, where the vessel was brought out from the sea and placed on a dry platform in order to be inspected and repaired. During these repair works, some worn panels on the deck plating were replaced with new ones, but without attention given to their proper thickness. The old panels had a thickness of 16mm, while the new ones had 14mm or even 12mm in some parts of the structure. The commission concluded that the difference in thickness of the panels was inappropriate according to the standards that should be followed during dry dock. Furthermore, the maintenance did not include inspections through NDT methods, even in the more susceptible sections of the hull, and the details of the work that had been done were not recorded in official documents.

The ballast tanks are the number one weakness factor for tanker ships, with age and overall condition, similar to that of the Erika. These tanks are usually made up of thin, uncoated steel panels that allow corrosion to develop and put the structural integrity at risk. Corrosion can also affect adjacent ballast tanks due to the heat conducted through the tanks caused by the nature of the cargo, leading to condensation. The parts of the ship that are particularly vulnerable to failure are the longitudinal plates, which could affect the ship's structure. Combining the existing corrosion with the aforementioned defective repairs, especially the thickness of the new plates, it is obvious that corrosion could be a significant factor in the failure.

The conversion of some cargo tanks into separate ballast tanks caused a redistribution of applied stresses on the structure, affecting structural sections such as bulkheads that are subject to overstresses. Hence, the bulkheads between the tanks of the ship could easily fail, resulting in cargo displacement and a different distribution of applied forces. Regarding the loading of heavy oil, the commission verified that it was not a reason for failure because the cargo was well allocated in the tanks, and the bending moment and shear force had allowable values according to safety limits, while the ship was not overloaded.

Considering the aforementioned factors, the initial list of the ship was caused by water ingress through a large crack that propagated at the side shell plating of the hull due to the failure of transverse webs. These webs fractured due to the breaching of the longitudinal bulkhead between the No. 3 center cargo tank and the No. 2 starboard ballast tank. The rapid propagation of the crack led to the aggravation of the vessel's condition, bringing about the final rupture. The commission came to a conclusion that the cause of the accident was the fracture of these transverse webs of the starboard ballast tank. It was undoubtedly considered that the crack spreading at the longitudinal bulkhead, triggered by the loss of rigidity of transverse webs through their subject to buckling, led to the weakness of at least one transverse web. As the hydrodynamic forces continued to gradually increase, the web frames began to fail due to distortion.

8.3.2 Conclusion

The commission concluded that the sinking of the ship was due to the tensile stresses applied at the bottom of the hull, affecting the longitudinal bending moment, which was near the maximum safety margin. It should be noted that the ship's hull was weakened due to the collapse of the bulkhead and the damaged side shell plating. The existing cracks in the side plating started to propagate at the bottom of the hull, leading to the inevitable total breakage of the vessel.

The Erika disaster can be attributed to structural failure, which began with the fracture of the longitudinal bulkhead between the No. 3 cargo tank and No. 2 starboard ballast tank, resulting in the rupture of the transverse webs of No. 2 tank. The failure of the transverse webs caused wide cracking of the side shell plating and subsequent propagation at the bottom section of the structure, where the final fracture was inevitable. The weakness of the structure, particularly at the No. 2 ballast tank, had developed due to insufficient maintenance and extensive corrosion, leading to a succession of failures causing the final rupture. Hence, corrosion was considered the root cause of the accident as it was the primary damage mechanism, while the other reasons were deemed subordinate.

The commission stated that in order to prevent such accidents in the future, all the involved parties such as the international organizations, the classification societies, the ship owners, the flag states, and the charters should ensure that the vessels are well-maintained and inspected. They should give high priority to the tanks that are susceptible to corrosion attacks and ensure a more frequent period of surveys, including several measurements such as the strength of the hull and the thickness of the plates [67].

8.4 M/T Prestige

The M/T Prestige, a 26-year-old single-hull ship registered in the Bahamas, broke apart and eventually sank on November 19, 2002, causing a severe environmental disaster on the northwest coast of Spain due to the oil spill that resulted from the shipwreck. The ship was carrying 76,972 tons of oil at the time of the accident. It had started its route on October 31 with the final destination of the Gibraltar straits, loading oil from intermediate terminals during its voyage. The ship measured 243.49m in overall length, 34.41m in breadth, and 18.70m in depth.

On the evening of November 13, the ship was hit by a large wave followed by a loud sound, causing the ship to suddenly list 20 degrees to the starboard (right) side, and the loading oil began to leak from the ship's tanks. The failure was assessed to have initiated from the 3rd starboard wing tank and rapidly developed to the 2nd starboard tank, possibly through the bulkhead that was between the two adjacent tanks. The crew abandoned the ship safely except for three officers who tried to save the vessel. After multiple attempts and refusals from the authorities to tow the ship near the Spanish coasts, the ship was towed to a calm sea region. However, the hull's status deteriorated while a huge amount of oil leaked into the sea. The consequences of the Prestige oil spill were significant, affecting the coasts of three countries: Spain, France, and Portugal.

Figure 56: M/T Prestige off the coast of Spain after break off in two.

Retrieved from: https://www.theguardian.com/world/2013/nov/13/spanish-prestige-oil-tanker-disaster

The root causes of the accident were considered to be the damage caused by Ship-to-Ship (STS) operations, fatigue, stresses due to large amount of new metal welded at old metal plates and corrosion.

8.4.1 The Failure

The most likely reason that triggered the failure of the ship was the large wave that struck the structure due to the heavy storm. The wave impact caused a crack and deformation at the side shell of the 3rd starboard wing tank. The 2nd and 3rd tanks were empty during the voyage, and the wave's influence led to the emergence of the hull's weaknesses. After the cracking of the 3rd tank, the increased internal pressure, in conjunction with the deformation that had occurred, resulted in breaching the bulkhead between the two tanks and water ingress. The initial failure originated in an empty ballast tank and could have been the result of several damage mechanisms.

Figure 57: The ship at the early stage of the failure.

Retrieved from: [68]

The damage that was caused by the contact due to STS could be one factor. The ship had operated as a mother ship for a period of four months, meaning it was a floating store where ships loaded and unloaded their oil cargo. Because of the fact that the ship had come into contact several times with other vessels, the structural integrity was always at stake, and there was a risk for damage to the side shells. At the time of the accident, through witness material, mainly photographs, two points with permanent deformation at the side shell of the ship's hull were detected, which could result in reduced strength at longitudinal panels and stiffened members. Thus, it was estimated that the 3rd starboard wing tank could have preexisted damage, and the frames could have gradually failed. Nevertheless, it was highlighted that this factor could be a reason that led to fracture but could not be the root cause of the accident.

Figure 58: The damage of the starboard side and the preexisting permanent deformations from STS operations at the side shell plating.

Retrieved from: [68]

Overstressing of the hull is a major concern that could cause several issues in the structure. According to calculations conducted by the responsible officers, the bending moment and the shear force were at safety levels during the ship's departure. The effect of the overstressing could be caused by the overpressure or underpressure in the tanks of the ship owing to the pumping of oil or ballast water. Nonetheless, this type of failure could have been prevented due to the visible deformation on the decks. Hence, it was reckoned impossible that the overstress of the hull during cargo operations could bring about hull failure.

Fatigue is not an abnormal effect in tanker ships. This type of failure leads to small crack lengths that may not justify the rapid entry of water, as only significant crack lengths result in such devastating outcomes. The creation of an unstable fracture characterized by a critical length and high spreading pace is connected with brittle fracture, which can lead to fatigue and fast propagation of the crack, justifying this damage mechanism. The possibility of fatigue failure of the 3rd starboard wing tank was investigated by ABS. Given that the ship had a 26-year lifetime, the vessel had not fulfilled the current fatigue standards required by the classification society. According to ABS, fatigue is a factor of failure that, under certain circumstances, is able to result in a fracture, but it was considered to be a contributing factor to failure and not the root cause of the incident.

Many longitudinal frames had been replaced one year before the accident, and extensive maintenance works had taken place to restore the ship. However, it is uncertain how the repeated repairs on such a wide scale could have led to reduced strength of the structure. It is known that residual stresses can bring about unstable fractures. The joint between new steel and old, corroded steel could cause a stress concentration region at their connection point, leading to several consequences for hull integrity.

Corrosion is an important issue for ships and one of the most challenging difficulties in the shipping industry. In a special survey conducted in 2001, it was found that a significant amount of the steel in the 3rd starboard tank had corroded extremely, exceeding safety margins. In order to pass the survey, the corroded steel was chipped off so that the steelwork could meet the appropriate limits, but more steel was cropped than necessary, resulting in a significant reduction in the thickness of the steel plates. The period between the inspection and the accident was 18 months, which was sufficient time for corrosion to propagate, especially when the structure is uncoated like the 3rd tank. Although it was impossible to evaluate how much of the steelwork thickness had been reduced due to corrosion, the corrosion was not considered the root cause of the failure.

8.4.2 Conclusion

The investigation report concluded that it was not possible to detect a specific root cause of the accident that could be the decisive factor for the initial failure. However, the aforementioned damage mechanisms (contact damage due to stress, fatigue, poor steel replacement, and corrosion) were considered to have acted individually or in combination to cause the fracture of the 3rd starboard wing tank. After the accident, some standards associated with fatigue and extensive repairs, primarily due to residual stresses, were reviewed to prevent similar accidents in the future [68].

8.5 MOL Comfort

The container ship MOL Comfort, with a capacity of 8000 TEU, was built by Mitsubishi Heavy Industries in Nagasaki, Japan, in 2008. It departed from Singapore on June 11th, 2013, with its first stop in Jeddah, Saudi Arabia, as the initial port on a long journey. The ship carried 4382 containers, which equals 7041 TEU, and had a crew consisting of 26 people. The ship flew a Bahamian flag and measured approximately 316m in length, 45.6m in beam, 25m in depth, and 14.5m in draft. Its cruising speed was 25.25 knots. The Japan Bureau, Class NK, classified the ship.

Figure 59: The container ship MOL Comfort.

Retrieved from: https://www.shiplilly.com/blog/mol-comfort-sinks-shocking-images/

The ship consisted of seven cargo holds in front of the engine room and two cargo holds aft of the engine room. It was the sixth in a series of large container ships, meaning that the shipping company had six sister ships sharing the same design. On the morning of June 17th, 2013, the wind was blowing at a speed of 38 knots (19.5m/s) - approximately 7 on the Beaufort scale - and the waves were 6m high and 100m long, while the ship was traveling at 17 knots. At 07:45 local time (GMT+5), 430 nautical miles off Oman, the ship was struck by two large waves in quick succession, and suddenly behaved unusually, specifically in a hogging condition. Following an investigation by the crew responsible for ensuring structural safety, it was reported that cargo hold No. 6 sustained severe damage and experienced extensive water ingress. The ship sustained a fracture amidships, causing it to break into two halves. At 09:45, the crew safely abandoned the ship.

Figure 60: MOL Comfort after the failure of her hull.

Retrieved from: https://gcaptain.com/mol-comfort-incident-photos/

The aft part of the ship, which was carrying 1,700 containers and 1,500 tons of fuel, sank almost immediately after being fully separated. The fore part of the ship remained afloat, and attempts were made to tow it. However, a wildfire broke out onboard, and the fore part eventually sank at 19:00 UTC on July 10th, 2013, carrying the remaining 2,400 containers and 1,600 tons of fuel. The technical investigation of the disaster was assigned to the bureau responsible for the ship (Class NK), the Committee on the Safety of Large Container Ships, and the International Association of Classification Societies (IACS).

(a)

(b)

Figure 61: (a) The aft part of the ship, (b) The fore part.

Retrieved from: https://gcaptain.com/mol-comfort-incident-photos/

The ship was built according to Class NK standards, which is a member of IACS. The investigation concluded that the ship's design was in accordance with predetermined rules from the regulatory authority. The total loss of the ship, as it sank to depths between 3000 and 4000 meters, exacerbated the failure analysis of the accident because it was impossible to conduct testing and experiments on the fracture and the affected structure region. Furthermore, a factor that aggravated the investigation was the total loss of recording archives. The investigation was based on interviews, including the possibility of the human factor, as the crew could have been in an unstable psychological condition, Noon Reports, Voyage Planning documents, and weather data.

After examinations that took place on the other five sister ships of MOL Comfort, preventative measures were taken until the root causes of the accident came to light. Therefore, actions were taken to reduce the stress on the hull, and some advanced work was carried out to ensure extra strengthening of the hull structure, resulting in double the strength compared to the initial structure, which was deemed acceptable according to safety standards. Lloyd's Register expressed the opinion that the structural reinforcement was the best preventative measure that could be taken [69].

8.5.1 The Failure

The ship, while sailing, was hit by two waves that caused a fracture in the hull amidships. The ship was subjected to a hogging condition, which is defined as the convex deformation of the hull in the longitudinal direction. The observed fracture was considered to have initiated from the bottom of the ship, the part that was submerged into the sea, and propagated along the structure, leading to the upper deck as the point of fracture that failed last. The fracture that cut the ship in two halves was assumed to have initiated from the No.6 cargo hold bottom shell plates.

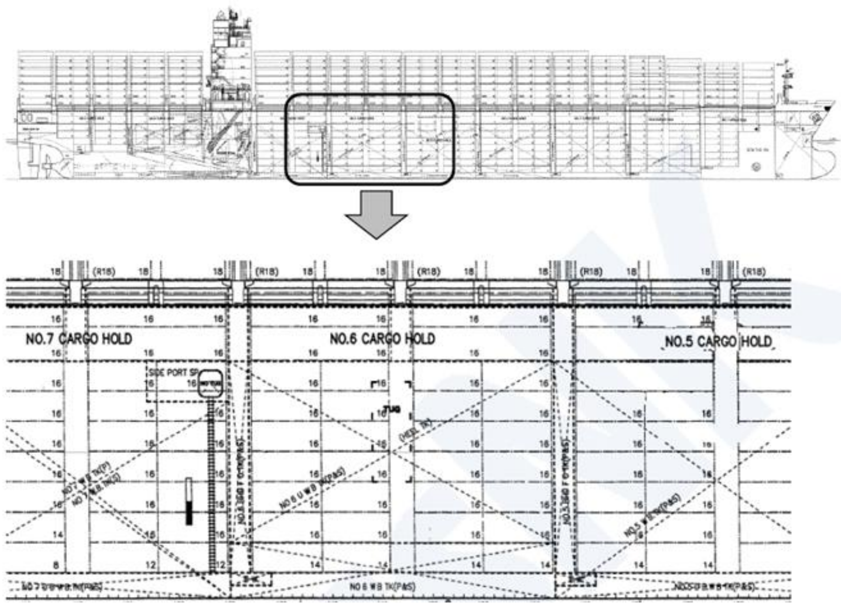

Figure 62: Ship design and the layout of the midship part.

Retrieved from: Class NK Investigation report [71].

The investigation used three methods to calculate the data that the report will use to draw conclusions about the accident. The Japan Bureau, Class NK, which was responsible for the ship, used three different methods to analyze the margin of the hull strength. These three methods include: the IACS URS11, which relates to longitudinal strength standards and considers vertical bending strength, the IACS CSR or Smith's method, which is based on Common Structural Rules released by IACS, and a 3-hold elasto-plastic analysis model.

It is estimated that the hull strength of the ship was $14.0\ x\ 10^6\ kN * m$. On the other hand, the loads that were acting at the hull were $9.4\ x\ 10^6\ kN * m$, which is almost 67% of the hull strength under the specific sea condition that dominated at the time of the accident. It was found that the ship had resisted loads under different sea states until $10.0\ x\ 10^6\ kN * m$ during voyages three and a half years before the failure. Hence, there are three possible explanations for the occurrence:

- The magnitude of actual loads that acted on the ship during the incidence exceeded the estimated loads.
- The hull strength was reduced at the time of the accident due to buckling phenomena that led to deformations of the bottom plates
- A combination of the aforementioned factors

The investigation used evidence from the Sister Ships of the MOL Comfort and from the ships that are characterized as Post-Panamax ships, which are a category of ships to which the Mol Comfort and her sister ships belong. The sister ships appear to have a permanent deformation of about 20mm on the bottom shell plates along the welded regions where the different blocks of the ship were joined during the prefabrication process to create the total hull of the ship. However, it was impossible to conduct simulations that took into consideration the 20mm buckling deformation, and these deformations could not occur even if the applied loads were narrow to hull strength. Therefore, it was imperative to detect the root cause of the buckling deformation of the bottom shell plates.

It is important to follow a procedure that includes all possible causes of the failure, based on the conditions that existed during the accident. The possible causes can be found in the following table:

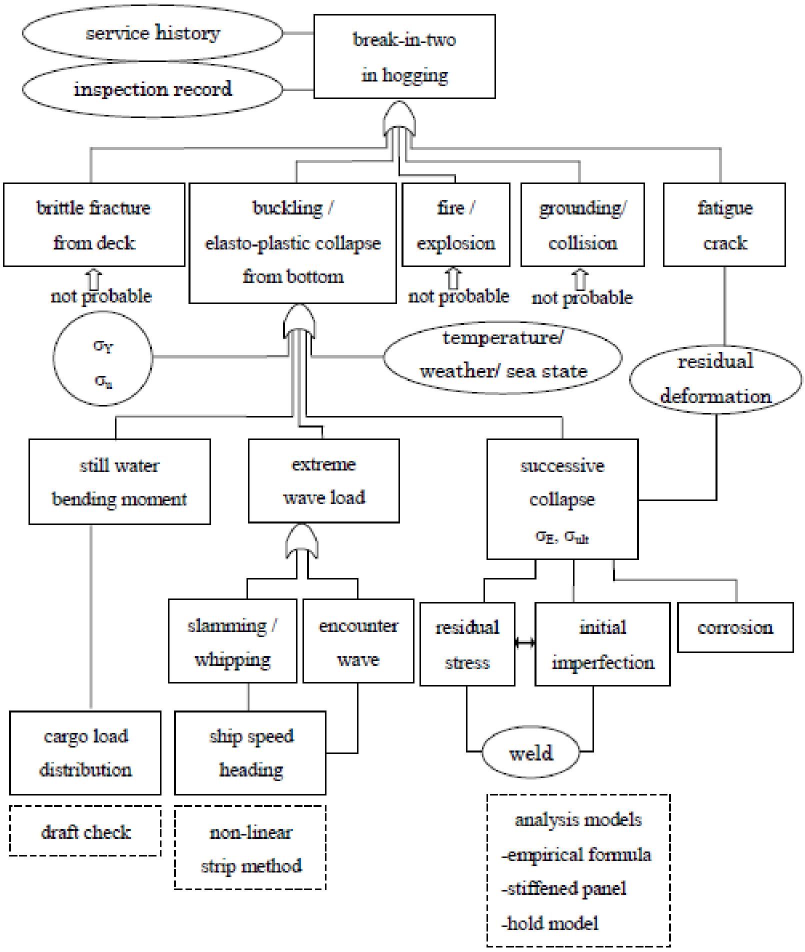

Figure 63: An analysis of possible failure factors.

Retrieved from: Committee on Large Container Ship Safety, Interim Report, Japan, December 2013 [70].

The investigation led to the conclusion that brittle fracture could not have occurred on the upper deck of the ship because the fracture had started from the bottom decks of the ship. Furthermore, scenarios involving grounding, collision, fire, or explosion were clearly ruled out. Among the remaining root causes, the scenario of buckling of bottom shell plates was considered to be the prevailing cause, which could occur when the load applied to the hull girder exceeds its strength (ultimate strength).

Furthermore, considering the loads that acted on the hull girder, the still water bending moment was estimated based on the weight distribution along the ship, and the wave loads were evaluated depending on the ship's speed, course, and sea conditions. The data regarding the weight of the containers onboard the ship were based on information provided by the operator. Additionally, corrosion was excluded from the investigation as the ship had only been operational for five years, and no damage from corrosion had been recorded during inspections. On the other hand, fatigue was considered a major factor in the failure, as it can affect welded structures such as ships.

The ship was built using YP47 steel (yield stress $460\frac{N}{mm^2}$) and the hatch coaming was extensively used not only to prevent water ingress but also to mitigate the toughness reduction caused by the utilization of thicker plates. The fuel tanks were designed as a part of the double hull and placed in a predetermined location in accordance with the rules to prevent environmental accidents. Water ingress was first detected at the centerline of the double bottom. Subsequently, extensive water ingress was detected at cargo hold No. 6. As shown in the Figure 64, the crack originated from the bottom of the ship and reached the upper deck. Therefore, simulations were conducted to assess the load applied to the bottom shell plates amidships in order to determine how the crack started and propagated, ultimately resulting in the total fracture of the hull.

Figure 64: The fractured hull of the ship.

Retrieved from: https://gcaptain.com/mol-comfort-incident-photos/

Regarding the deformations that were detected on the sister ships, it was decided to reinforce the hull strength as a preventative measure. The investigation showed that the deformation occurs at the welded parts between the blocks that form the hull. After inspections were carried out on the sister ships, the welding quality of the bottom shell plates was found to be adequate according to standards, leading to the conclusion that fatigue may not have contributed to the failure of the MOL Comfort [70].

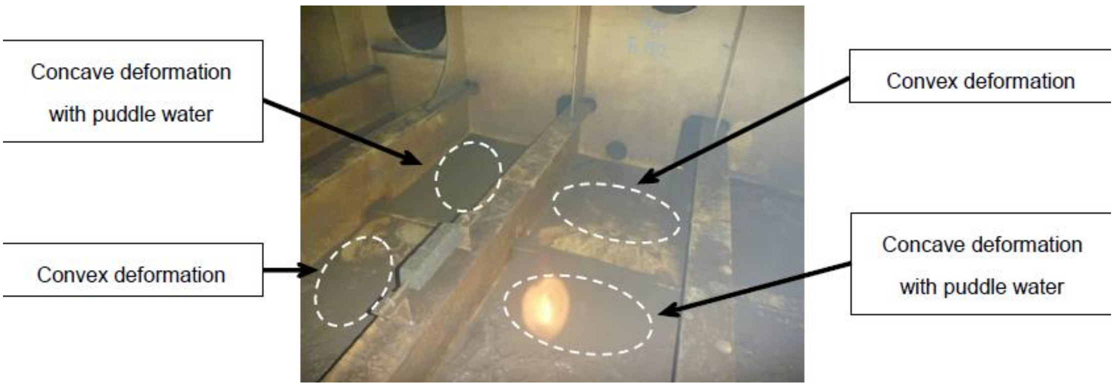

Figure 65: Buckling deformation in the bottom shell plates of the sister ships.

Retrieved from: Committee on Large Container Ship Safety, Interim Report, Japan, December 2013 [70].

The interim report indicated that the hull girder ultimate strength estimated from the evidence was 150% of the assessed vertical bending moment at the time of the accident. Hence, it cannot be assumed as a factor that could lead to fracture. The report also showed that there is a need to specify a series of uncertain factors related to the strength and the load applied to the hull. These factors related to strength are:

- Yield stress
- Influence of residual stresses due to welding
- Lateral loads (sea pressure and the pressure that containers act) at bottom shell plates (local deformations)

The factors related to loads are:

- Sea conditions
- Affection of vertical bending moment due to the weight distribution

To estimate the hull strength at the time of the accident, two cases were suggested. Case 1 refers to the minimum yield stress of the hull based on deviations in the mill sheet values of the ship. Case 2 includes the minimum yield stress given by Class NK. The effects of local deformations applied to the bottom shell plates, the hull girder ultimate strength, and the residual stresses at the welded regions in the separate blocks of the ship, in the longitudinal direction, could have had an impact on the accident because there was a chance that the load of the vertical bending moment could surpass the hull's ultimate strength. Nonetheless, these two margins are close enough. The wave-induced load was estimated considering 27 different sea states at the time of the accident, combining three separate wave heights (5.5, 6.5, and 7.5m) with mean periods of 10.3, 12.5, and 15.5 seconds, and three possible wave directions (120, 150, and 180 degrees)

The upper limit of the wave-induced vertical bending moment was calculated based on the aforementioned conditions and was found to be $7.23\ x\ 10^6\ kN * m$. The still water bending moment was estimated based on the container weights declared by the shippers, resulting in $6\ x\ 10^6\ kN * m$. Considering a 10% increment, which was evaluated based on the values of sister ships during their departure, the sum of the aforementioned vertical moments is $13.8\ x\ 10^6\ kN * m$. Meanwhile, case 1 estimates $13\ x\ 10^6\ kN * m$ and case 2 $12\ x\ 10^6\ kN * m$ as a lower limit of the hull strength. In addition, it was found that local deformations that acted on the bottom plates can reduce the ultimate strength of the hull by a maximum of 4%, and the influence of welding on the longitudinal bottom plates can reduce the ultimate strength by a maximum of 5%. At the time of the accident, there was a possibility that the upper limit of the applied loads would exceed the lower limit of the strength, resulting in a fracture.

Regarding the double bottom structure and the margin of the strength, no differences were found between the MOL Comfort and other container ships that belong to the same category with respect to the margins that were implemented by IACS UR S11 and the hull ultimate strength IACS CSR. However, the effect of lateral loads on the double bottom structure was not taken into account. In the case of considering the existence of these loads, the 3-hold elasto-plastic analysis model detected a significant difference between the MOL Comfort and other reference ships. As a consequence, Class NK concluded that the strength of the double bottom structure against lateral loads, such as sea pressure and container weight, is related to the hull ultimate strength in the event of the accident.

Regarding the effect of buckling collapse strength of the bottom plates, the Japan Bureau investigated this critical value depending on three loads that act on these plates under two conditions. The three loads are the compressive ones in the longitudinal direction due to the vertical bending moment at the hogging condition, the upward lateral loads due to the sea pressure applied at the bottom of the hull, and the compressive loads in the transverse direction resulting from the sea pressure acting at the sides of the ship. The two conditions that are important in facilitating the investigation of the possibility of failure are the margins of strength against the existing loads and the level of deviation. Class NK concluded that the bottom shell plates had undergone plastic deformation in the transverse direction directly before the ship reached the maximum load of the longitudinal hull girders. From the moment that the bottom plates were locally buckled and failed under plastic deformation, the effective plating breadth diminished, and as a result, the compressive stresses acting on the girder caused by lateral loads gradually increased. As a result of these extreme compressive stresses, the down half of the girder was plastically deformed, so the resistance of the double bottom strength against the sea pressure and container weight was decreased, leading to the growth of buckling collapse of the bottom shell plates, bringing about the hull fracture.

It is noteworthy that, after a wide investigation, there were no accidents in the past where the buckling collapse of the bottom plates was the root cause of the failure. The knowledge gained from the case study of MOL Comfort was significant as it highlights some factors that, under certain circumstances, could lead to fracture:

- The local strength of the double bottom, such as the one developed against the loads that are acted upon by the sea and containers in the transverse direction, is closely associated with the hull girder ultimate strength regarding the buckling collapse of bottom plates.
- The double hull of the ship is subjected to loads that are acted upon due to the sea pressure. Under these circumstances, there is a possibility that the local buckling collapse could bring about a strength reduction of the hull girder due to the superimposition of the vertical bending moment.
- The hull structural strength can be estimated adequately enough by taking into consideration the hull girder fracture, but only when the hull girder ultimate strength is assessed considering the effects of the lateral loads.

8.5.2 Conclusion

The investigation concluded the following points:

- There is a possibility that the load vertical moment could have exceeded the hull's ultimate strength at the time of the accident if uncertain factors, such as yield stress, sea states, and the deviation between the declared and actual weights of containers onboard, are taken into consideration.
- There are significant differences regarding the hull's ultimate strength, as per the 3-hold elasto-plastic analysis model, between MOL Comfort and other reference ships when considering the local stresses that lead to buckling collapse of the stiffened bottom panels due to lateral loads and compressive stresses due to vertical bending moments.

Nevertheless, uncertainties persist as it cannot be determined with clarity how the fracture at the bottom of the ship initiated and propagated so quickly. Container ships, while the market demands increase rapidly, transport more and more loads and are continuously evolving by increasing their length (>300m), speed, and critical design characteristics such as large hatch openings on the deck. As a result, the ship is subjected to slamming, which can cause extreme vibrations at the hull and hydrostatic effects that wear out the hull structure. Considering these effects and the slamming that can cause stress amidships with a magnitude equal to that caused by wave-induced stress, the outcome is a doubling of the vertical bending moment at the middle of the ship's structure. Assuming that MOL Comfort was in a hogging condition according to her 'ureau, Class NK, it was not impossible for the scenario of the buckling of stiffened plates to occur, which could lead to extensive plastic deformation.

Another factor that remains uncertain is how the buckling of the plates was triggered and how the crack propagated so quickly. If there was a crack or flaw at the welded regions or in the vicinity of these areas, which is normal in welded structures like ships, the aforementioned stresses (lateral loads) could lead to the growth of the crack. Furthermore, the vibrations from slamming and wave-induced movements of the hull create alternate stresses at the crack. In combination with other load conditions such as low cycle fatigue and an unstable state of the crack, these vibrations could directly lead to a large crack in the transverse direction of the bottom plates before the crack's expansion. This scenario matches the general observation of the occurrence because the steel that the ship was made of can resist fast fracture unless the crack is long enough.

8.5.3 Recommendations

In order to confirm the structural safety of sister ships and other ships belonging to the same category as MOL Comfort (Post-Panamax 8000 TEUs), it is imperative to estimate the hull girder strength based on a 3-hold elasto-plastic model that considers the effects of lateral loads. Additionally, an important preventive measure is to assess the critical buckling value of the stiffened bottom plates amidships, which is the part of the hull where the ship undergoes significant stresses.

Regarding the current standards of Class NK, the main points that are important to notice are the development of a practical method to estimate the hull girder's ultimate strength, taking into consideration the impact of lateral loads. Additionally, the procedures related to the transverse strength of the hull must be checked, and possible modifications may need to be implemented. Furthermore, research on finding a method for calculating wave-induced and whipping damage, caused by rapid flexing of the hull girder, needs to be expanded. Finally, new methods for designing and implementing hull monitoring systems can help reduce the possibility of similar accidents occurring in the future [71],[72].

8.6 VLOC Stellar Daisy

On 31st March 2017, the Very Large Ore Carrier (VLOC) Stellar Daisy, with a capacity of 266,141 deadweight (DWT), was sunk during its route from Brazil to Qingdao, China. During the accident, the ship was sailing in the South Atlantic Ocean and was approximately 1,700 nautical miles away from the coasts of Uruguay. The depth of the sea at that location was about 3,500m. Onboard the ship, there were 24 crew members, but only 2 managed to survive the disaster and be rescued safely. The Republic of the Marshall Islands Maritime Administrator was charged with carrying out an investigation in order to find the root causes of the failure. The commission that was appointed concluded that the most likely reason for the ship's founder was a significant 45° list that followed a devastating structural failure, leading to extensive flooding of the separate compartments of the vessel and the final loss of buoyancy.

Figure 66: The VLOC Stellar Daisy.

Retrieved from: https://www.bbc.com/news/world-latin-america-39475836

The failure had probably begun from the No. 2 Port Ballast Tank. The reason for the fracture of the ship was a combination of damage mechanisms that deteriorated the structural condition of the ship over time. Material fatigue, corrosion, permanent defects, multi-port discharges, and weather conditions that the ship had to withstand between her departure and the accident led to a significant reduction in the ship's hull strength. The ship was a single-hull ship and was built as a Very Large Crude Carrier (VLCC) in 1993 at Mitsubishi Heavy Industries in Japan. The ship was designed, constructed, and supervised according to Class NK standards. The steel that was used for critical sections of the ship was steel grade AH, which was mainly utilized for decks, side and bottom shell plating, as well as longitudinal and horizontal girders. Steel grade AH36 was used for the longitudinal bulkheads between the tanks and the vertical stiffeners that support the bulkheads. In 2008, the ship underwent an extensive conversion from VLCC to VLOC, which was a major endeavor not only from an engineering perspective but also from the standpoint of standards and rules that should have included requirements for such wide modifications.

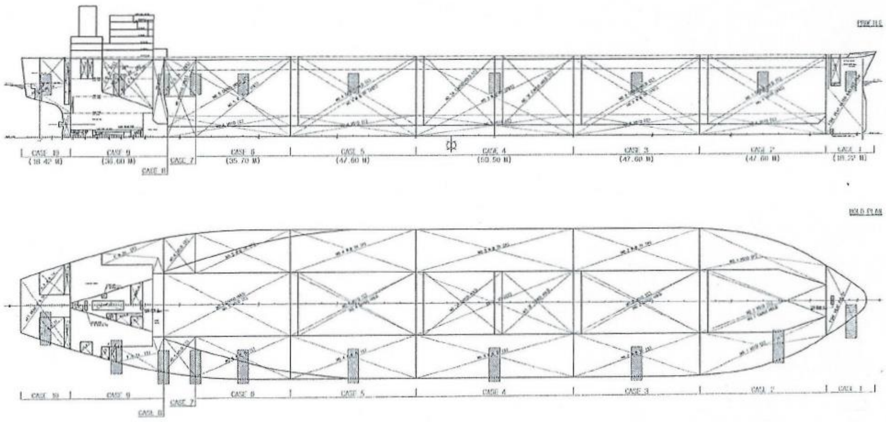

Figure 67: The modified ship design.

Retrieved from: [73]

8.6.1 The Failure

The commission tried to identify the root causes of the accident by investigating all possible factors that may have contributed to the structural failure. Due to the high density of the ore cargo, there is a potential for poor distribution of weight. The distribution of weight plays a crucial role as it can lead to structural failure in case of wrong estimation of bending moments and shear force, which should be within the maximum safety limits. According to the report, the bending moment and shear force had allowable values due to the departure of the vessel, and it was considered impossible for them to exceed the safety margin during the voyage of the ship. Even though there were no documents verifying the acting of longitudinal loads on the hull of the ship.

The weather conditions during the journey of the Stellar Daisy were severe but not abnormal for this region, with wind speeds of about 7-8 Beaufort and waves of 6-7 meters in height. The combination of waves and swells could lead to simultaneous rolling, which would subject the hull to high stresses. Under these conditions, the ship's structure should resist the dynamic loads, as it has done in the past. However, due to the weakened strength of the hull, the application of these loads could cause a failure more easily. Changing the course of the ship may help avoid the rolling and hull strain, but it cannot be said with certainty whether this change could save the ship due to the lack of available data.

The ship was built in 1993 with an expected lifetime of 20 years. As the ship aged, the hull underwent fatigue due to cyclic loads that were applied during its operational life. After being modified into a VLOC, the vessel consisted of a large amount of new steel, but there was still an important quantity of the original metal in the structure that had not been removed or renewed. The old steel of the ship, after 15 years of operating as a VLCC and another 8 years as a VLOC, was susceptible to fatigue, as there were some critical points that could develop cracks. Vital parts of the ship, such as the side and bottom shell plating, and deck longitudinals, had end connections made with the original steel. During the previous dry docks and inspections of the ballast tanks, 58 cracks were identified at the bottom longitudinals and 73 at the side shell plating.

The loss of material due to corrosion attack affects structural members by reducing their rigidity, making them flexible, and increasing their potential to fail. Corrosion can also create voids or notches that lead to stress concentration points. Ballast tanks are especially prone to corrosion, so they should be coated and fitted with anodes. During dry dock inspections, any corrosion found in the ballast tanks identified and repaired. However, according to the Master's reports from 2016, the protective coating layer of the ballast tanks was severely damaged, as well as the anodes that had been fitted. Ballast tanks are affected by corrosion not only due to the presence of oxygen but also because seawater is loaded into them to ensure the ship's stability. Thus, corrosion is considered a significant contributor to the failure of the ballast tanks.

During the dry docks of the Stellar Daisy, extensive repairs were carried out in order to keep the vessel in compliance with safety standards and classification requirements. Most of the work involved cutting away damaged or corroded metal and replacing it with new material. Although welding old and new steel is a common practice, it can cause regions with concentrated stresses and reduce the elasticity of the steel at the heat-affected zone (HAZ) of the weld. These stresses can lead to crack initiation and propagation due to fatigue and have the potential to evolve into large breaches. Additionally, repairs to the frames on the side shell and deck longitudinals involved the insertion of extensions that were sometimes shorter and less precise than they should have been. While the repair work provided essential reinforcement to the structural members, it also created regions with high concentrations of stress, making the hull structure more susceptible to rupture.

Another reason that contributed to the catastrophic structural failure of the vessel was multi-port unloading. The ship’s stability and loading reference book did not include any standards for partially loading and sailing in short coastal distances (approximately 20-25 nautical miles), which the ship did during 2016 and 2017. The commission indicated that this multi-port discharging with such great frequency led to overstress of the hull and probably caused local deformations at stress-concentrated areas.

The commission stated that the reduction in the strength of the ship's hull was due to a combination of damage mechanisms, such as fatigue, corrosion, structural repairs, and frequent unloading. The most probable sequence of failures during the ship's sinking was the fracture of the structural members, which resulted in uncontrolled water ingress and the loss of buoyancy. These members failed because of the existing fatigue cracks in the No. 2 and No. 3 port ballast tanks and their rapid propagation at the bottom shell plating, resulting in a fast entry of water. Furthermore, the fast and progressive fracture of the transverse members of the structure and the presence of cracks at the main deck caused uncontrolled flooding in the port-side ballast and cargo tanks. The last section of the ship to fail was the bulkheads between the tanks, which led to the release of the cargo and the flooding of the accommodation apartments.

8.6.2 Conclusion

The ship sank due to a 45° list following the destructive failure of her hull, resulting in the loss of buoyancy and excessive water ingress. The structural failure was considered to have initiated from the No. 2 port ballast tank and spread rapidly to the adjacent port ballast tank No. 3. The total loss of structural integrity was a combination of factors. Supplementary reasons for the failure could be detected during the conversion repairs when the ship was modified into a VLOC, and the installation of larger ballast tanks increased the possibility of structural failure when one of them flooded. Additionally, there were gaps in SOLAS requirements regarding the exact placement of longitudinal bulkheads, which could prevent uncontrolled flooding in the event of water ingress in one cargo or ballast tank while the ship was at a laden condition [73].

8.7 Sea Gem

In 1964, British Petroleum (BP) decided to begin oil extraction activities in a more productive way by converting a 12-year-old American barge into a 10-leg oil rig and equipped it with all the necessary apparatus to begin drilling the oil reservoirs underneath the sea floor in the British approved zones. The offshore platform was about 75.3m long, 27.4m wide, 3.96m deep, and had an operating height of 15.24m. It was named as the Sea Gem. On September 30, 1965, it was transferred and installed at blocks in the North Sea, where an economically exploitable gas deposit was found. Until October 12, the operation of the drilling rig was without any interruptions, and during the inspections, no flaws or defects were detected that could cause concerns about the structural integrity of the platform. Some usual repairs were conducted at the tie-bars and jacks, but these were due to routine maintenance.

Figure 68: The Sea Gem platform.

Retrieved from: http://www.energyglobalnews.com/december-1965-the-sea-gem-sanks-and-becomes-the-first-oilfield-tragedy-of-the-north-sea/

On November 23, however, a tie-bar on one leg of the rig broke, fortunately causing no damage to the leg, and it was immediately replaced by a spare. The crew inspected the tie-bars mounted on the other legs but did not find any concerning cracks or similar issues. Hence, the operations continued at the same pace as before the incident. During some inspections that took place in mid-December, attempts were made to lift the supporting legs, but some of them got stuck in the sea floor, leading to the decision to give up the operation of maintenance and examination of the legs. On December 22, the legs were eventually lifted, but not enough to be inspected. The side effect of this attempt was that by lifting the legs, all the weight of the platform was distributed dissimilarly compared to the other legs. On December 27, the Sea Gem underwent a jacking operation to be lowered by 3.05 m, with the intent of moving it to a different location. During this operation, the front jacks moved as expected, whereas the mid and tail jacks did not. No obvious reason for this was determined, and the senior operator decided to release air from the front jacks so that the rig could return to its initial position. Shortly after these actions, the front starboard supporting legs failed, resulting in the sinking of the platform and the loss of 19 workers out of the total 32.

8.7.1 The Failure

At the time of the accident, the temperature was about 3°C, the winds were light, and the waves were about 3m in height. The investigation that was carried out to identify the root causes of the accident indicated that the accident was a consequence of the collapse of the tie-bars, which led to the overstress that the structure was subjected to. The fracture analysis of the ruptured tie-bars indicated the existence of brittle breaching, notches, defects due to welding, and fatigue cracks. The conditions under which the Sea Gem collapsed facilitated its susceptibility to the damage mechanism of brittle fracture.

The offshore platform underwent cyclic loads during its operational life due not only to the hydrostatic forces coming from extreme weather conditions such as heavy winds and waves but also from its drilling operation, which inevitably generated vibrations that deteriorated the status of the rig and made it prone to fatigue. The operating company had not taken into consideration the contribution of wave loading in the North Sea, resulting in mistaken calculations of the loads that applied in that region. After some time, these loads could cause small cracks that can propagate and lead to total failure.

Brittle fracture was the decisive factor in the failure of the platform. The steel that was used for the construction of the rig experienced a ductile-to-brittle transition temperature (DBTT), which caused it to lose its elasticity and resulted in a rapid and sudden fracture. According to the Charpy Test, which took into account the water temperature, the tie-bars exhibited brittle fracture under the yield stress.

8.7.2 Conclusion

The outcome of the disaster revealed some major issues that must be considered by the offshore industry. The protection of the jacks against severe weather conditions and the development of a new type of steel that can resist low temperatures and the DBTT phenomenon were the first steps toward safer drilling operations. Additionally, the Sea Gem was a pioneering force in the gas-oil industry at that time, and its demise led to groundbreaking changes in terms of oil rig safety and structural integrity regulations. The new laws and standards that were enacted placed the highest priority on the safety of human life during offshore activities. The commission that conducted the investigation stated that fatigue in the tie-bars used to connect the legs with the platform's structure, and brittle fractures caused by freezing temperatures, led to this catastrophe [74],[75].

8.8 Alexander L. Kielland

The Alexander L. Kielland platform was one of eleven semi-submersible oil rigs built following the French Pentagon design between 1969 and 1977. The different parts of the platform were constructed at German and French yards, while the process of assembling these parts was carried out at CFEM yards in Dunkirk. In 1976, the platform was delivered to its Norwegian owners and placed approximately 320km from the east coast of Scotland in Norwegian waters. The rig was owned by the Stavanger Drilling Company of Norway, while the operator during the accident was a U.S. company named Phillips Petroleum. Although the platform was built for oil extraction activities, it had never been used for this purpose. Instead, it was used as a floating hotel to accommodate personnel working in the offshore industry in this region. Initially, the platform was designed to accommodate 80 people, but after some modifications in 1978, the capacity increased to 348 people by adding extra spaces in the pipe stand area.

Figure 69: The Alexander L. Kielland offshore platform.

Retrieved from: https://en.wikipedia.org/wiki/Alexander_L._Kielland_%28platform%29

The platform had a weight of 10.105 tons and had dimensions of 103m x 99m, with a depth of 40.5m from the upper deck to the base of the columns. Five pontoons, each with a diameter of 22m, and five columns, each with a height of 8.5m, were connected by a complex mesh consisting of horizontal and diagonal bracings with a tubular shape. These supporting structures had diameters of 2.6m and 2.2m, respectively, while the steel used was 25mm thick. The lower decks were made from thinner steel. However, designers did not include bracings between the B and C columns or the C and D columns because they believed it would be infeasible for supply vessels to approach the platform. The upper and diagonal braces were waterproof, while the lower horizontal supports were susceptible to water ingress.

In order to gather information about the position of the platform, transponders were installed on the seabed, and hydrophones were installed underneath the three lower horizontal bracings and the D6 support. The installation process required cutting the structural support and placing a tubular steel, which was then welded with a double-fillet weld to provide support for the hydrophone instrument.

On the evening of March 27th, 1980, 212 off-duty personnel were resting on the accommodation platform. At the time of the accident, the platform was near the production jacket at the Edda field. The weather conditions were characterized by an wind speed of about 7-8 on the Beaufort scale (16-20 m/s) and significant wave heights of about 6-8m. Shortly before the accident, people witnessed the feeling of a sharp crack and a shivering motion. Five out of six cables that stabilized the platform, ensuring its safety, broke from the seafloor, leaving only one to prevent the Alexander L. Kielland from capsizing. The rig reached a slope of 30°, putting its stability at stake. Many issues emerged during the evacuation procedure as the lifeboats and the overall process proved insufficient due to design deficiencies. The remaining cable prevented the capsize for about 14 minutes and eventually broke, leading to the devastating accident. Out of the 212 people onboard, only 89 managed to survive the accident.

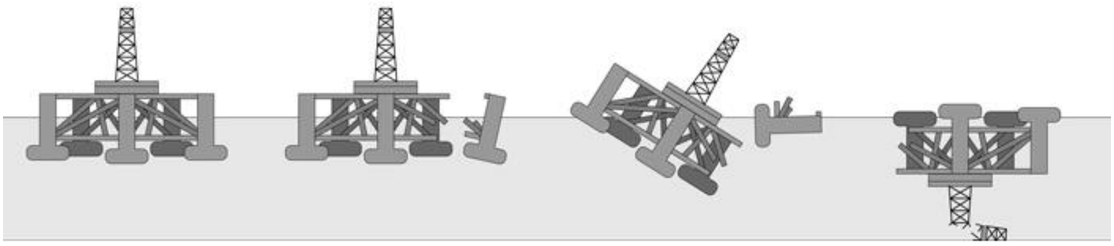

Figure 70: The sequence of events at the moment of the failure leading to the capsizing of the platform.

Retrieved from: https://www.idunn.no/doi/full/10.18261/issn.2387-5879-2019-01-11

The investigation into the accident was carried out by the Commission of Inquiry, as mandated by the Royal Decree. This was clearly the worst accident to have occurred in Norwegian history since World War II. Given the importance of the accident, Norway urgently sought to identify the root causes of this failure in order to reconstruct the services responsible for supervising offshore activities. The accident marks the worst industrial accident in Norway's history. Despite the Commission's indisputable opinion that the failure originated from column D, which separated first from the structure, leading to the rig's capsize 20 minutes later, the Commission conducted a deep examination of the broken columns of the platform and conducted chemical, metallurgical, mechanical, and fracture analysis research to release the report on the failure one year later.

8.8.1 The Failure

The investigation, from its early steps, resulted in the finding that the root cause of the failure of the D6 brace was fatigue at the double-fillet weld, which joined the hydrophone support with this brace. The platform’s complex supporting network led to the failure of all the braces that were connected to column D because of the rapid and sudden application of external overloading forces, resulting in the failure of leg D.

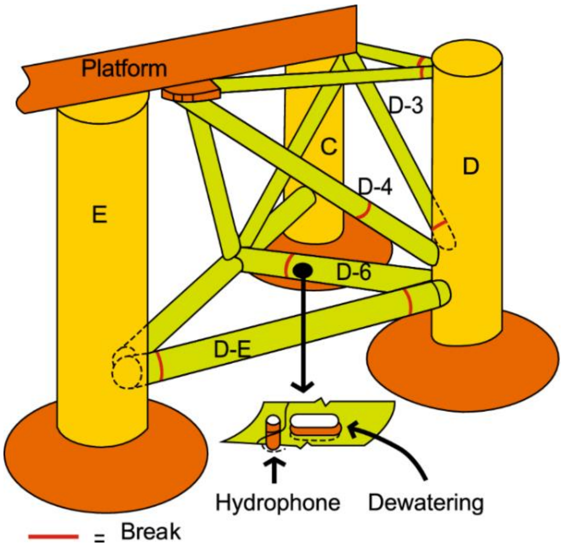

Figure 71: Position of fatigue fracture on D6 brace.

Retrieved from: https://link.springer.com/article/10.1007/s11668-019-00680-4

The initiation and propagation of the crack were strongly accelerated due to the existence of flaws inside the double-fillet weld between the hydrophone mount and the brace. After the stage that was related to the initiation of the crack, the crack grew and spread through the cross-section of the brace along the two sides of the hydrophone support. From the first examination of leg D's fractured surface, marks were detected that indicated fatigue as the damage mechanism that caused the accident. These marks were associated with a sharp and clean fracture surface with minimal plastic deformation and a clean beach mark pattern that emerged from the hydrophone penetration. The final fracture of the D6 brace was brittle, while the other braces that were joined to column D failed due to their inability to withstand the overload that arose after the absence of the D6 brace.

Although fatigue was the main reason for the failed brace that led to destabilization and gave rise to the platform catastrophe, a wider investigation at the hydrophone mount showed that some fractures had occurred prior to the fracture that caused the failure. These fractured surfaces were the result of extensive corrosion attack on parts of the circumference of the tube. It is important to highlight that the double-fillet weld was cracked for more than 75% of the circumference. Moreover, some areas of the fractured surfaces showed marks of the presence of lamellar tearing that had occurred during welding and was due to the poor through-thickness ductility of the material in the hydrophone tube. Additionally, after fractography analysis, it was found that the fracture occurred 1mm near the HAZ, a fact that implies that high-strength steels used for such welded structures were affected by the diffusion of H_2 at the crack's tip and could cause hydrogen embrittlement, bringing about an increased pace of propagation and high residual stresses due to the welding process.

The general appearance of the fractured surfaces showed the existence of a thick layer of corrosion products above the surface of the tube. Nevertheless, the cathodic protection worked adequately as a preventative measure against corrosion attacks, implying that these products had accumulated for years before the moment of the accident. This assumption was verified by samples from paints that were found on the fractured surfaces and proved that the double-fillet weld of D6 had already been cracked before the platform was launched. Except for D6 fatigue failure, all the other fractures in the braces that connected to the column were due to overloading, resulting in the formation of ductile characteristics such as coarse and fibrous appearances.

Regarding the material of the platform, the steel that was used was found from documents and coincides with Lloyd's Register of Shipping grade EH steel. After the accident, many tests were performed using specimens from the brace and mount. The outcomes of these tests indicated that, regarding the chemical composition, the materials met the required specifications, and the Charpy tests (39J impact energy at -40°C) also met the specifications as the outcomes were normal for this type of steel. However, the Charpy tests for the hydrophone tube indicated much lower impact energy of 16-17J at -40°C. Another concern emerged from the low yield point of the D6 support (343-346 MPa), while the specified minimum margin was 353MPa. Similarly low values related to yield points were received from the other braces. The tests that were performed to define the ultimate strength and elongation indicated that the braces surpassed the minimum required values.

The through-thickness ductility of the D6 brace was not taken into consideration, and it was also inadequate. The values found for the D6 material fluctuate between 5% and 13%, and the ultimate strength ranges between 419 MPa and 459 MPa. Although there were no requirements for ductility, the ultimate strength was low enough compared to the specified minimum safety margin of 501 MPa in the transverse direction. The importance of through-thickness ductility lies in the vulnerability to lamellar tearing fracture in welded plates. The specifications for the minimum limits that ensure safety, according to DNV classification standards for offshore structures, is a 20% reduction in area, but this fluctuates according to weld type and process, so in other designs, this percentage is between 15-30%. In the pentagon design of the Alexander L. Kielland platform, the hydrophone support was not considered as part of the structure, resulting in the absence of the application of material quality requirements.

The hydrophone support had a similar chemical composition and strength to D6, but its ductility in the thickness direction fluctuated between 1-5%. The low value of this property is mainly due to the large amount of slag inclusions, which consisted of manganese, sulfide, and a small quantity of aluminum oxides in banded perlite and ferrite microstructure. Therefore, the low strength and ductility of the hydrophone tube material, in conjunction with poor welding quality, led to partial cracking of the double-fillet weld immediately after construction and before the platform became operational. In addition, the high loads from the external forces applied due to the severe environmental conditions in which the platform had to operate caused rapid crack growth. These external loads were estimated based on the wind speed and wave information provided at the time of the accident. After processing this data, the stresses that the offshore structure was subjected to were assessed as follows:

- Stresses at Stillwater condition: 73 MPa
- Stress amplitude due to wave impact: 60-100 MPa

The sum of the influence of these stresses is 131-173 MPa. Although these stresses are only 50% of the yield stress, their contribution was magnified due to the hydrophone tube acting as a part of the structure, which increased the total magnitude of the stresses.

8.8.2 Conclusion

After conducting tests in the laboratory and analyzing the structure, the commission appointed to investigate the accident concluded that there were insufficient material properties in the hydrophone tube. They highlighted the poor through-thickness property and poor welding quality, which led to partial cracking of the double-fillet weld that joined the tube with the D6 support. In addition to that, the deficiencies that existed in the structure before it was put into service, in combination with fractures caused by corrosion attacks, led to the distribution of stresses and aggravated their impact on the structure, ultimately affecting its strength under fatigue. Fatigue is responsible for 2/3 of the circumferential fractures, including the stages in which the crack initiated and propagated, while the remaining third is due to the unstable condition of the crack. The failure of the other braces of column D was due to overloading.

The inspections were inadequate, and during the construction and maintenance of the offshore structure, they failed to reveal the flaws and cracks necessary to prevent the accident. Another significant fact is that damage tolerance, especially in welded structures, was not considered as design criterion in Alexander L. Kielland's design, and there were no specifications regarding residual strength.

Thus, fatigue depends on uncertain factors related to the environment in which the operation takes place and the loads that are applied. This, combined with the limited inspections and the lack of reliability during inspections of large welded offshore structures, suggests that residual strength should be taken into account when considering a damage tolerance analysis procedure. This accident was the motivation for changing the design standards and redefining the rules for offshore structures [76], [77].

9. Conclusion

Summarizing the thesis, it can be concluded that marine structures, which are large all-welded structures, are designed to operate in harsh environments. The main failures that have been analyzed in this thesis are ductile fracture, brittle fracture, corrosion, and fatigue. These damage mechanisms could have significant consequences on the structural integrity of marine structures, leading to devastating effects such as environmental disasters, human casualties, and economic losses.

To prevent these failures, materials have been developed in order to resist the aforementioned failure mechanisms. The steel industry has developed new processes such as the Thermo Mechanical Control Process (TMCP), which produces high-toughness steels and allows large heat input welding. The introduction of YP40 steel (yield strength 390MPa) has led to increased strength and reduced overall ship weight. EH47 steel is widely used in container ships to ensure the high strength of certain parts of the ship, as well as high toughness and crack restraint that are necessary at hatch-side coaming around the openings of the decks where the loading and unloading process takes place. To prevent brittle fracture, the critical factor K_C should be between 4000-6000 $\frac{N}{mm^{1.5}}$, considering the standards of the classification societies. Every possible crack that propagates from the welded joint part at the base metal will be restrained due to the adequate toughness of the material. Thus, sufficient prevention of cracks is ensured by preventing brittle fracture and high toughness for important structural members [78].

Corrosion, as one of the biggest challenges of the shipping industry, has been addressed by using sacrificial anodes and an advanced system called Impressed Current Cathodic Protection (ICCP). This system provides essential hull protection from corrosion by ensuring the minimum potential difference and generating the opposite current to the physical corrosion current in order to protect the anode from corrosion attack. The metal that needs protection is connected with an indissoluble anode, and the current passes to the opposite current via a DC source. Therefore, the corroding metal is converted from anode to cathode and eventually protected from corrosion in the long term [79].

Marine structures are welded constructions designed to operate with a lifetime of 20-25 years, considering the extreme loads to which they are subjected. Therefore, fatigue is a type of failure that could affect the structural integrity in the long term. For this purpose, NDT methods have been developed to detect cracks and restrain their propagation. Additionally, the state of the material's surface is significant. A smooth surface lacking geometric discontinuities leads to an increased lifetime of the structure, while corrosion and poor mechanical working of the materials can bring about its diminished lifetime. Welded structures are known to have initial flaws. Hence, in order to address the fatigue issue and increase the structure's lifetime, damage tolerance analysis is followed by keeping the crack propagation pace reduced by using coarse-grained materials.

In order to ensure the safety of marine structures and prevent accidents, it is necessary to follow the rules and standards set by classification societies. The objective of these societies is to certify the strength and structural integrity of critical components, such as a ship's hull, and to ensure the reliability of the systems installed on vessels. The Bureau inspects ships and offshore structures from the moment of their design plans to construction and during their operation through periodic surveys.

The International Maritime Organization (IMO), as a statutory classification organization, is responsible for ensuring that minimum standards are met for marine structures, especially ships, in order to be accepted in countries other than the country in which they are registered. These requirements include rules and regulations such as SOLAS Ch II-1, which specifies the design, construction, and maintenance requirements for structural, mechanical, and electrical components [80].

The shipping industry is a global industry that is responsible for 90% of worldwide transportation. Therefore, rules and standards have been established and modified to ensure structural safety and prevent accidents. The knowledge and research gained from previous failures should serve as a compass for a more advanced, reliable and safer industry in the future.

References

[1] Donald J. Wulpi, Understanding How components fail, 3rd edition, ASM International, Ohio, 2013

[4] B.Hayes, Engineering Failure Analysis, Vol 3 (1996) 115-127

[6] Bernt S. Aadnoy , Reza Looyeh, Petroleum rock mechanics, 2nd edition 2019, pp53-62

[7] John Case M.A, F.R.Ae.S, Lord Chilver M.A.D.Sc., F.Eng., F.R.S., Carl T.F. Ross B.Sc., Ph.D, D.Sc., C.Eng., Strength of Materials and Structures, 4th edition 1999, pp94-151

[11] U.S. Department of Energy, Material Science, DOE Fundamentals Handbook, Vol 2, 1993

[12] Beer, Hohnston, DeWolf, Mazurek, Mechanics of Materials, 7th edition, Mc Graw-Hill, New York, 2015

[18] Charles K.Harley, The shift from sailing ships to steamships, 1850-1890: a study in technological change and its diffusion, 2006

[19] Paulet, Dominique, Architecture navale, connaissance et pratique, Villette, Paris, 1999

[20] Eyres, D.J., Molland, A.F., Schneekluth, H. and Bertram, V, Shenoi, R.A. and Dodkins, A.R., Watson, D.G.M, The Maritime Engineering Reference Book (2008), pp636,638-727

[22] Ge Wang, John S.Spencer, Sittha Saidarsamoot, Swieng Thuanboon, David L.Olson, Brajendra Mishra, Handbook of Environmental Degradation of Materials, 2nd edition, pp799-832

[24] Ravichandran, K., Ship Breaking Industry: Key Trends and Credit Implications, 2012

[26] Tomi Solakivi, Tuomas Kiiski, Tuulia Kuusinen, Lauri Ojala, Journal Of Cleaner Production , Vol 294, 2021

[27] James F.Wilson, Encyclopedia of Physical Science and Technology, 3rd edition 2003, pp161-168

[29] K. Sadeghi, GAU J. Soc, Appl.Sci., 2(4) 2007, pp1-16

[31] Mohamed A., El-Reedy, Offshore Structures, GPP, 2012

[32] Bader Diab, Naji Tahan, Handbook of Offshore Engineering, 2005, pp1055-1126

[35] Ann Scarboroug Bull, Milton S.Love , Ocean and Coastal Management, Vol168 2019, pp274-306

[36] Royal Academy of Engineering report:

https://raeng.org.uk/media/b0ebnlfo/raeng_offshore_decommissioning_report.pdf

[37] A. Pineau, T.Pardoen, Comprehensive Structural Integrity, Vol 2, 2007, pp709-757

[38] K.J. Rawson and E.C. Tupper, Basic Ship Theory, Vol 1, NTUA, 2002

[39] Papadopoulos Christos, Diploma Thesis ‘Study of the Hull Stresses of a Ship using the Method of Principal Stresses’ , NTUA, 2017

[40] Mohamed Shama, Buckling of Ship Structures, Springer, Alexandria, 2013

[41] Philippa Moore, Geoff Booth, The Welding Engineer’s Guide to Fracture and Fatigue, 2015, pp95-110

[42] Michael D. Hayes, Dale B.Edwards, Anand R. Shah, Fractography in Failure Analysis of Polymers, pp1-5, 6-22, 48-92

[43] N.Saba, M.Jawaid, M.T.H.Sultan, Mechanical and Physical Testing of Biocomposites, Fibre-Reinforced Composites and Hybrid Composites, 2019, pp1-12

[44] William D. Callister Jr, David G. Rethwisch,, Fundamentals of Materials Science and Engineering, John Willey and Sons, NJ, 2088

[45] Adrian P.Mouritz, Introduction to Aerospace Materials, 2012, pp454-468

[46] D.J. Abson and R.J. Pargeter, International Metal Reviews, vol31, 1986, pp141-196

[47] Dominique Francois, Handbook of Materials Behavior Models, 2001, pp566-576

[48] John J. Burke, Volker Weiss, Application of Fracture Mechanics to Design, Springer Science+Business Media, New York, 1979

[49] Pietro Pedeferri, Corrosion Science and Engineering, Springer, Switzerland,2018

[50] Aleksandrs Urbahs, Konstantins Savkovs, Gints Rijkuris, Darja Andrejeva, Transport and Aerospace Engineering, Vol 6, 2018, pp5-14

[51] Branko N. Popov, Corrosion Engineering, Elsevier, Amsterdam, 2015

[52] Yong Bai, Wei-Liang Jin, Marine Structural Design, 2016, pp477-487, 569-578

[53] Stephens, R.I., Fatemi, A., Stephens, R.R., Fuchs, H.O., Metal Fatigue in Engineering, 2nd edition, John Wiley and Sons, New York, 2000

[54] Suresh, S., Fatigue of Materials, 2nd Edition, Cambridge University Press, 1998

[55] Inge Lotsberg, Fatigue Design of Marine Structures, Cambridge University Press, 2016

[56] M. Ramulu, A.S. Kobayashi, Encyclopedia of Vibration, pp505-512

[57] Jwo Pan, Shih-Huang Lin, Fatigue Testing and Analysis, 2005, pp237-284

[58] Jorge Luis Gonzalez-Velazquez, Fractography and Failure Analysis, Springer, Mexico City, 2018

[60] Kobayashi H., Onoue H., Brittle fracture of Liberty Ships, https://www.shippai.org/fkd/en/hfen/HB1011020.pdf

[61] Kevin Kendall, Crack Control, 2021, pp1-29, pp137-163

[62] John Lancaster, Engineering Catastrophes, 3rd edition, 2005, pp139-189

[63] M.D. Harris, W.J. Grogg, A.Akoma, B.J. Hayes, R.F. Reidy, E.F. Imhoff, P.C. Collins, The Journal of The Minerals, Metals and Materials Society (TMS), Vol67, 2015, pp2965-2975

[64] Daniel J. Benac, Nicholas Cherolis, David Wood, Journal of Failure Analysis and Prevention, Vol16, 2016, pp55-66

[65] Wei Zhang, Challenges, Vol 7, issue 2, 2016

[67] BEA/mer, Report of the enquiry into the sinking of the Erika off the coasts of Brittany on December 1999

[68] The Bahamas Maritime Authority, Hull failure and loss of the Prestige, November 2004

[69] The Bahamas Maritime Authority, Report of the Investigation into the sinking of ‘’MOL Comfort’’ in the Indian Ocean, September 2015

[70] Committee on Large Container Ship Safety, Interim Report, Japan, December 2013

[71] Class NK, Investigation Report on Structural Safety of Large Container Ships, September 2014

[72] Xiaoli Jiang, What happened to the MOL Comfort, Research gate, 2016

[73] Republic of the Marshall Islands Maritime Administration, Stellar Daisy casualty investigation report, April 2019

[76] A. Almar-Naess, P.J. Haagensen, B. Lian, T. Moan, T. Simonsen, Journal of Energy Resources Technology, Vol 106, March 1984, pp24-31

[77] T. Moan, Case Histories in Offshore Engineering, International Centre for Mechanical Sciences, Vol 283, Springer, 1985, pp1-42

[78] Ryuji Uemori, Takehiro Inoue, Kazutoshi Ichikawa, Tetsuro Nose, Masaaki Fujioka, Masanori Minagawa, Hiroyuki Shirahata, Steels for Marine Transportation and Construction, Nippon Steel Technical Report No. 101, November 2012

Websites

[2] https://csengineermag.com/the-great-boston-molasses-tank-failure-of-1919/

[3] https://www.history.com/news/great-molasses-flood-science

[5] https://airwaysmag.com/aloha-airlines-flight-243/

[8] https://sdcverifier.com/articles/what-is-von-mises-stress/

[9] https://help.solidworks.com/2013/english/SolidWorks/Cworks/r_Maximum_von_Mises_Stress_Criterion.htm

[10] https://help.solidworks.com/2015/english/solidworks/cworks/r_maximum_shear_stress_criterion.htm

[13] https://help.solidworks.com/2021/English/SolidWorks/cworks/r_Maximum_Normal_Stress_Criterion.htm

[14] https://ojs.nassg.org/index.php/sms/index

[15] https://www.britannica.com/technology/ship/History-of-ships

[16] https://exploration.marinersmuseum.org/watercraft/phoenician-ships/

[17] https://www.hmy.com/a-timeline-of-ships-boats-and-yachts/

[21] https://www.marinelink.com/articles/maritime/shipbuilding--vessel-construction-100164

[23] https://www.shmgroup.com/blog/dry-dock-history-types-advantages-and-innovation/

[25] https://www.industriall-union.org/cleaning-up-ship-breaking-the-worlds-most-dangerous-job

[28] https://www.caralb.com/2021/05/31/offshore-platforms/

[30] https://www.tigergeneral.com/offshore-oil-gas-production-benefits-economy/

[33] https://www.sulzer.com/-/media/files/campaigns/res/offshorewhitepapercampaignthechallengesofmaintainingequipmentonoffshoreplatformswhitepaperpdfrender.ashx?la=en

[34] https://www.asme.org/topics-resources/content/the-afterlife-of-old-offshore-oil-rigs

[59] https://hrcak.srce.hr/file/161554

[66] https://www.twi-global.com/media-and-events/insights/world-concord-tanker

[74] https://werf-gusto.com/wp-content/uploads/2015/08/524-2055-1-PB.pdf

[75] http://www.dukeswoodoilmuseum.com/sea_gem.htm

[79] https://www.marineinsight.com/tech/hull-corrosion-and-impressed-current-cathodic-protection-iccp-on-ships-construction-and-working/

[80] https://iacs.org.uk/media/8875/classification-societies-key-role.pdf